Improvement of radiation shielding properties of some tellurovanadate based glasses

Yasser B Saddeek[1,2] , **Shams A M Issa**[2,3], **T Alharbi**[1], **H O Tekin**[4,5], **O Kilicoglu**[6], **T T Erguzel**[7], **K Aly**[2,8] **and Mahmoud Ahmad**[1,2]

[1] Physics Department, Collage of Science in Zulfi, Majmaah University, 11952, Saudi Arabia
[2] Physics Department, Faculty of Science, Al-Azhar University, Assiut 71452, Egypt
[3] Department of Physics, Faculty of Science, University of Tabuk, Tabuk, Saudi Arabia
[4] Department of Radiotherapy, Vocational School of Health Services, Uskudar University, Istanbul 34672, Turkey
[5] Medical Radiation Research Center (USMERA), Uskudar University, Istanbul 34672, Turkey
[6] Uskudar University, Vocational School of Health Services, Department of Nuclear Technology and Radiation Protection, Istanbul, Turkey
[7] Uskudar University, Faculty of Engineering and Natural Sciences, Department of Software Engineering, Istanbul, Turkey
[8] Physics Department, Faculty of Science and Arts Khulais, Jeddah University, Jeddah, Saudi Arabia

E-mail: y.mohamed@mu.edu.sa

CrossMark

Abstract

In this research, various valuable features having discriminating characteristics, namely the mass attenuation coefficient (μ_m), effective atomic number (Z_{eff}), energy absorption buildup factor (EABF), neutron removal cross-section (ΣR), mass stopping power (MSP) and projected range values were studied in the energy range of 0.015–15 MeV for vanado-telluride glass network had heavy or transition metal oxides. μ_m for the different glass series were calculated using Monte Carlo code. Besides, the EABFs were also calculated using geometric progression fitting technique. The proton and alpha MSP as well as projected range values were computed using SRIM code. Moreover, the generated μ_m by MCNPX for the different glass series was compared to the outputs of XMuDat and XCOM. The analysis indicated that the glass sample VTBi6 had good magnitudes of μ_m and the lowest values of half value layer, i.e. the sample had the superior radiation shielding properties among the explored glasses.

Keywords: mass attenuation coefficient, mass stopping power, tellurovanadate glasses

(Some figures may appear in colour only in the online journal)

Introduction

Radiation safety and protection studies, including gamma and neutron shielding are of increasing significance in a technologically developed society. The diversity of generated radioactive sources from nuclear power plants or the propagated used sources in several applications such as agricultural, energy and medicinal had increased the requirement to provide radiation shielding. The designing and production of an appropriate shield should include a diversity of parameters, such as shielding efficiency, thermal performance, easy use and cheap.

The researchers studied various types of different compound materials to be used as shielding materials due to their amenable structural properties [1–12]. The estimations pronounced ordinary concrete (OC) as heavy and non-transparent outclasses and the researchers dedicated to investigating glassy systems as radiation shielding materials [3–10].

Tellurite-vanadate oxide glasses have special and unique physical properties that vary with composition [11–13]. This
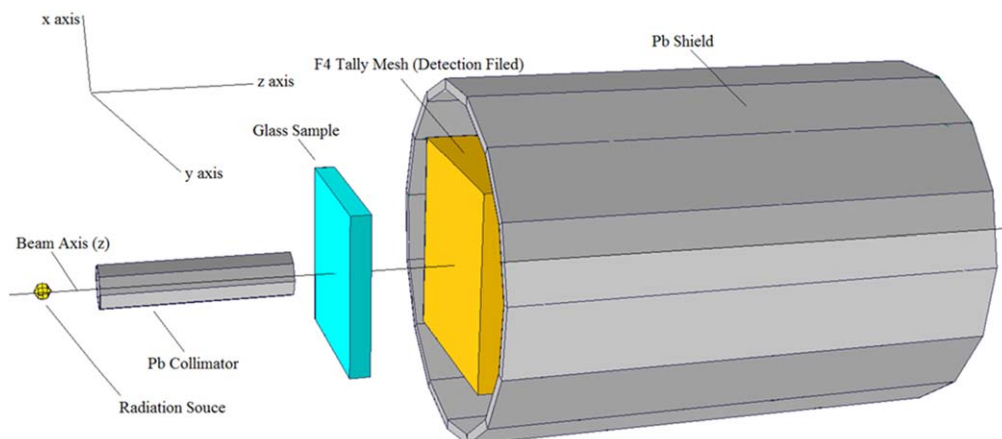
Figure 1. Simulation setup obtained from MCNPX Visual Editor.

Table 1. Fraction of element and density of glass samples.

Sample code	V_2O_5	TeO_2	TiO_2	Ag_2O	PbO	Bi_2O_3	Density (g cm^{-3}) [18]
(VTT)TiO$_2$-glass							
VTTi1	48	50	2	—	—	—	3.988
VTTI2	45	50	5	—	—	—	4.018
VTTi3	40	50	10	—	—	—	4.062
VTTi4	37.5	50	12.5	—	—	—	4.131
VTTi5	35	50	15	—	—	—	4.182
(VTAg) Ag$_2$O-glass							
VTAg1	42.7	53.6	—	3.7	—	—	4.469
VTAg2	38.4	54.1	—	7.5	—	—	4.795
VTAg3	33.9	54.7	—	11.4	—	—	5.094
VTAg4	29.4	55.3	—	15.3	—	—	5.368
VTAg5	24.7	55.9	—	19.4	—	—	5.720
(VTPb) PbO-glass							
VTPb1	47	53	—	—	0	—	3.996
VTPb2	42	54	—	—	4	—	4.240
VTPb3	38	54	—	—	8	—	4.510
VTPb4	34	54	—	—	12	—	4.807
VTPb5	29	55	—	—	16	—	5.133
VTPb6	24	56	—	—	20	—	5.383
(VTBi) Bi$_2$O$_3$-glass							
VTBi1	47	53	—	—	—	0	3.996
VTBi2	43	55	—	—	—	2	4.376
VTBi3	40	56	—	—	—	4	4.797
VTBi4	36	58	—	—	—	6	5.188
VTBi5	32	60	—	—	—	8	5.624
VTBi6	27	62	—	—	—	11	6.031

type of oxide glasses had suggested applications in antibacterial materials, solar cells and waveguides, heat pumps in photovoltaic panels, laser, photochromic glasses, radiation shielding and so forth [14]. High density, low-phonon energies, good stability and durability of tellurite-vanadate glasses can gave more insights for the determination of the effectiveness in reducing and attenuating different electromagnetic radiation of these glasses and to investigate the effect of irradiation on its mechanical and physical properties. For example, Elmahroug *et al* [15], El-Mallawany *et al* [16] and Tijani *et al* [17] examined potentiality of these glasses to be used as shielding materials. Moreover, the rigidity of the network of different tellurovanadate based glass series such as; VTT, VTAg, VTPb and VTBi was studied by ultrasonic
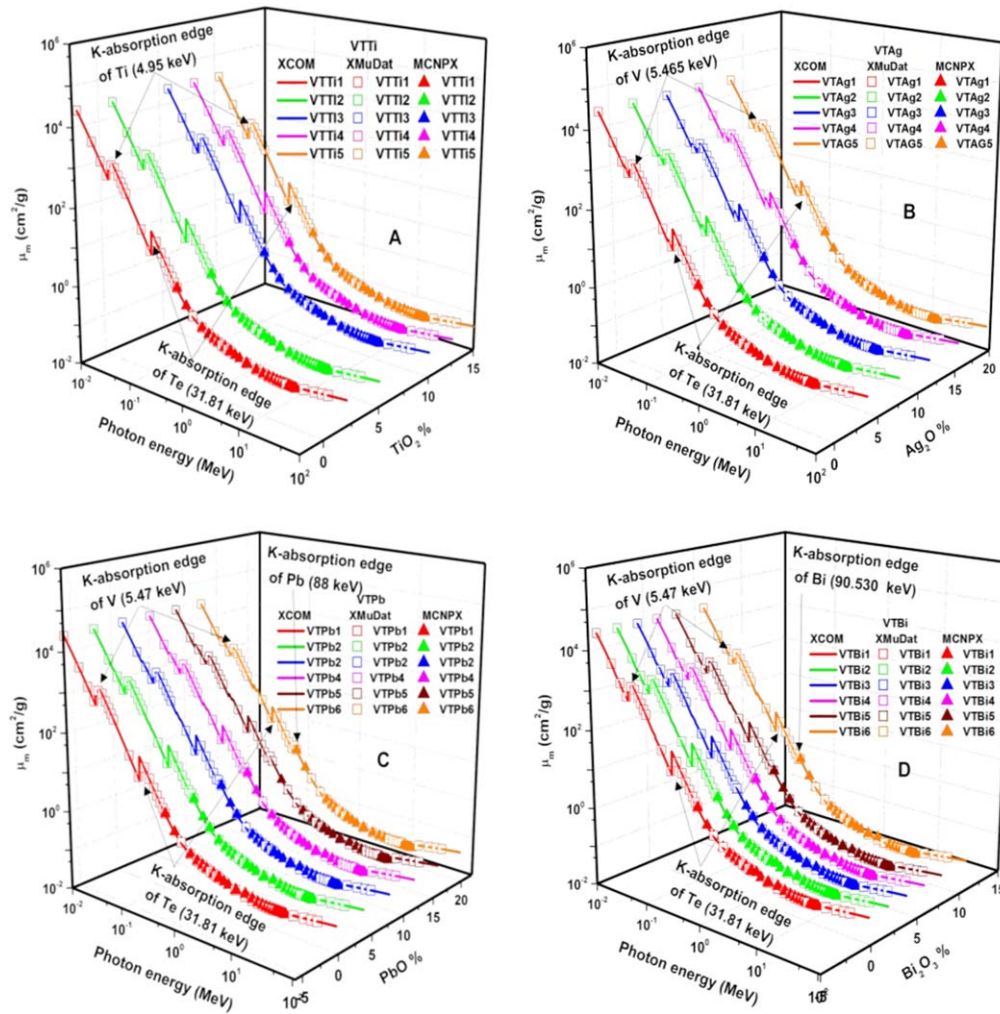
Figure 2. (A)–(D) XCOM mass attenuation coefficient (μ_{m}) value compared with XMuDat program and MCNPX code for investigated glass systems against photon energy.

technique to clarify the effect of the third oxide on the network [14].

In the field of nuclear radiation shielding applications, precision of the Z_{eff}, μ_{m}, half value layer (HVL), energy absorption buildup factor (EABF), ΣR, mass stopping power (MSP) and projected range are quite important and vital to the whole process. Thus, in this study, the μ_{m} of different tellurovanadate based glass series such as; V_2O_5–TeO_2–TiO_2 (VTTi), V_2O_5–TeO_2–Ag_2O (VTAg), V_2O_5–TeO_2–PbO (VTPb) and V_2O_5–TeO_2–Bi_2O_3 (VTBi); had been calculated using MCNPX code in the energy range 0.015–15 MeV. The importance of numerical methods such as Monte Carlo simulations in the field of radiation shielding is increasing rapidly. Among the well-known codes, the literature review has shown that MCNPX code was used for determination of shielding properties of different types of glasses. Therefore, we have utilized the MCNPX which is extended version of MCNP code since similar investigations using MCNPX code have been found in literature. The output of this code will be related to the outputs of XCOM and XMuDat. Besides, Z_{eff}, HVL, EABF, ΣR, MSP and the projected range of these glass series were also calculated. Table 1 tabulated the composition
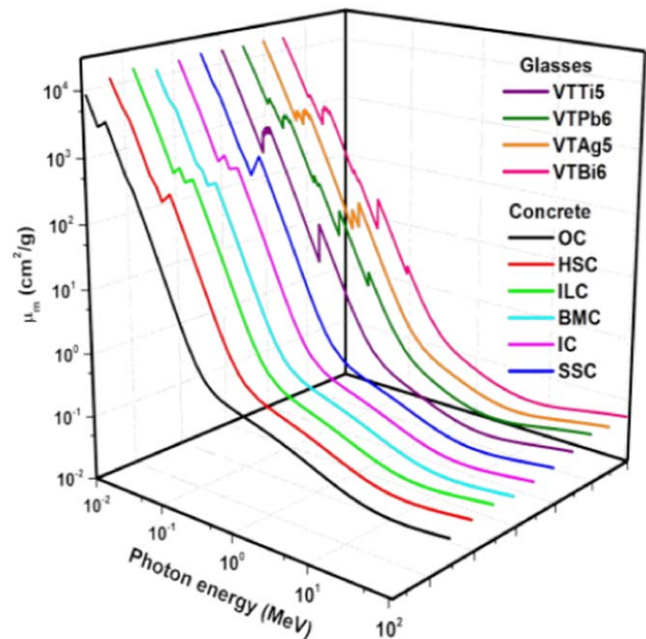

Figure 3. Mass attenuation coefficient for the VTTi5, VTAg5, VTPb6 and VTbi6 glass samples comparable to the μ_{m} values of different kinds of concretes.
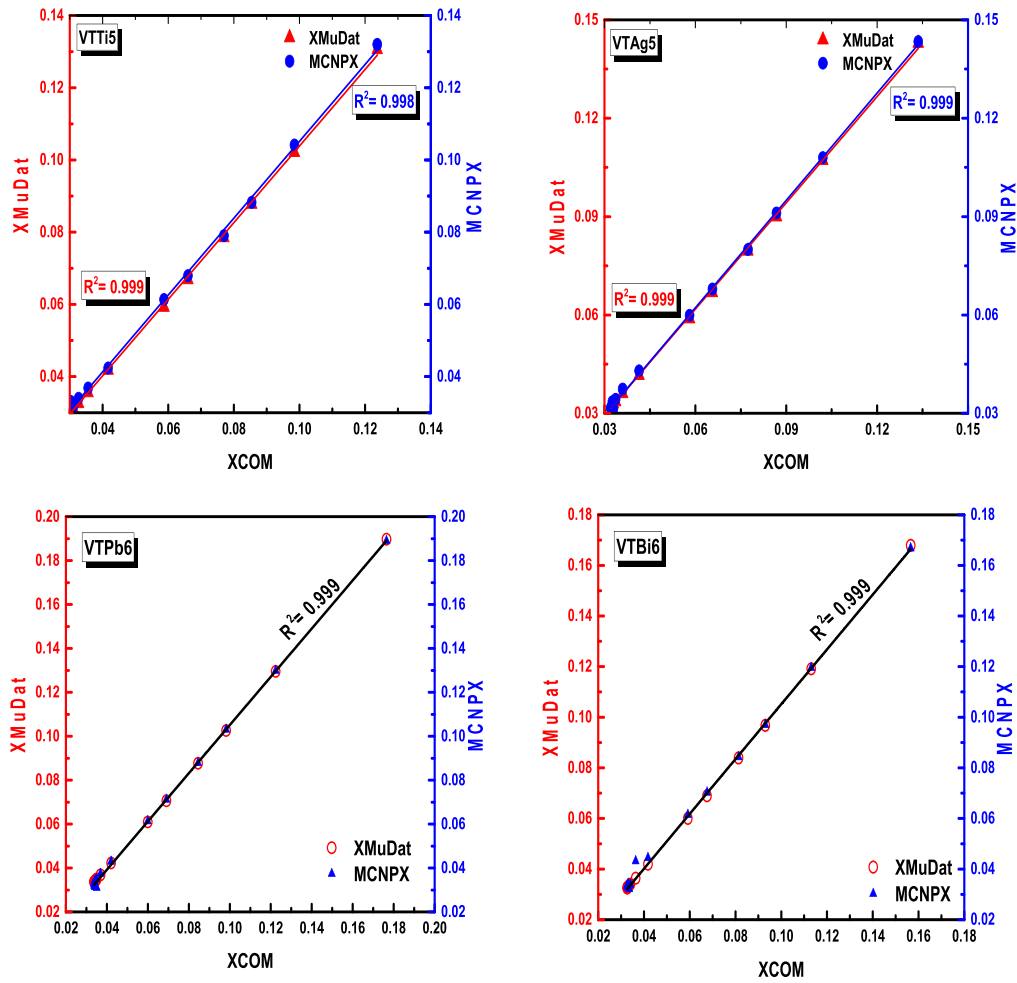
Figure 4. The correlation between the XCOM results and both XMuDat and MCNPX values for VTTi5, VTAg5, VTPb6 and VTbi6 glass samples.

of these glasses bedsides their densities. The results underline the impact of transition or heavy metal oxides on the network of tellurovanadte glasses. On the other hand, the results will contribute to the understanding of best radiation protection capability among the investigated chemical combinations.

Background

Gamma-ray attenuation for glasses was performed using narrow beam transmission geometry as shown in figure 1. A 3×3 inch NaI(TI) detector was used to measure the experimental μ_m values. The μ_m of the investigated glasses were obtained at an energy line 0.356 MeV, which emitted from ^{133}Ba radioactive sources. The diagram geometry of μ_m measurement is shown in figure 1. The Beer–Lambert law was used to evaluate the attenuated radiation (I) through the sample

$$I = I_o e^{-\mu t}, \qquad (1)$$

where I_o, μ, and t are the intensity of incident radiation, linear attenuation coefficient, and thickness of samples, respectively.

The magnitude of the intensity of a gamma ray is an important feature in the applications of radiation shielding. This intensity is reduced as it penetrates into any material by absorption or scattering. Decreasing the intensity of the gamma ray can also be possible by the change in the atomic number of the absorbing material. In radiation protection, scientists use the HVL to measure the intensity of the gamma ray. The HVL of a gamma ray is defined as the amount of shielding material that is required to reduce the beam to half of its original potential. HVL is used to measure whether there is enough liquidation in the gamma ray to remove low energy radiation, that is harmful, or not. It also helps to determine the type and thickness of shielding material being used for the facility. It is quite important to compare the magnitudes of HVL of the explored glasses with various kinds of concretes to clarify the radiation shielding capability of the explored glasses. So, the HVL values for VTTi, VTAg, VTPb and VTBi glass systems were compared to various types of concrete as shown in [19]. The gamma shielding capability of a specified substance may be gained by a definite parameter like the HVL. According to this parameter, the intensity of an incident photon was decreased to 50% of its origin based on the

Table 2. Mass attenuation coefficient (μ_m) using XCOM, XMuDat and MCNPX and their percent differences.

E (MeV)	VTTi1					VTTi2				
	XCOM	XMuDat	Δa	MCNPX	Δb	XCOM	XMuDat	Δa	MCNPX	Δb
0.1	0.7992	0.8497	6.13	0.8515	6.34	0.7991	0.8496	6.13	0.8524	6.45
0.2	0.1991	0.2146	7.49	0.2146	7.47	0.1991	0.2146	7.49	0.2159	8.09
0.3	0.1236	0.1305	5.43	0.1315	6.19	0.1236	0.1306	5.51	0.1316	6.25
0.4	0.0984	0.1021	3.69	0.1034	5.00	0.0984	0.1021	3.67	0.1035	5.07
0.5	0.0854	0.0877	2.67	0.0879	2.96	0.0854	0.0877	2.67	0.0879	2.96
0.6	0.0769	0.0785	1.97	0.0789	2.47	0.0770	0.0785	1.96	0.0789	2.47
0.8	0.0660	0.0668	1.28	0.0674	2.25	0.0660	0.0668	1.27	0.0675	2.34
1.0	0.0587	0.0592	0.90	0.0597	1.83	0.0587	0.0592	0.90	0.0599	2.06
2.0	0.0417	0.0418	0.22	0.0420	0.68	0.0417	0.0418	0.19	0.0420	0.68
3.0	0.0356	0.0355	0.11	0.0358	0.63	0.0356	0.0355	0.14	0.0358	0.61
4.0	0.0327	0.0325	0.46	0.0335	2.67	0.0327	0.0325	0.43	0.0337	3.01
5.0	0.0311	0.0310	0.29	0.0316	1.49	0.0311	0.0310	0.29	0.0316	1.53
6.0	0.0303	0.0302	0.23	0.0313	3.25	0.0303	0.0302	0.26	0.0314	3.61
7.0	0.0299	0.0298	0.37	0.0300	0.54	0.0299	0.0298	0.37	0.0301	0.91
8.0	0.0297	0.0296	0.34	0.0299	0.59	0.0297	0.0296	0.30	0.0299	0.69
9.0	0.0297	0.0296	0.27	0.0298	0.31	0.0297	0.0296	0.24	0.0299	0.58
10.0	0.0298	0.0297	0.13	0.0296	0.57	0.0298	0.0298	0.13	0.0298	0.03

E (MeV)	VTTi3					VTTi4				
0.1	0.7989	0.8494	6.13	0.8524	6.48	0.7988	0.8493	6.13	0.8528	6.54
0.2	0.1991	0.2146	7.49	0.2159	8.10	0.1991	0.2146	7.49	0.2162	8.24
0.3	0.1236	0.1306	5.51	0.1317	6.31	0.1237	0.1306	5.43	0.1319	6.41
0.4	0.0984	0.1021	3.65	0.1038	5.27	0.0985	0.1021	3.64	0.1040	5.44
0.5	0.0854	0.0877	2.68	0.0880	3.00	0.0854	0.0877	2.68	0.0881	3.14
0.6	0.0770	0.0785	1.96	0.0789	2.48	0.0770	0.0785	1.96	0.0789	2.52
0.8	0.0660	0.0668	1.26	0.0677	2.52	0.0660	0.0668	1.26	0.0679	2.79
1.0	0.0587	0.0592	0.90	0.0599	2.05	0.0587	0.0592	0.90	0.0601	2.40
2.0	0.0417	0.0418	0.22	0.0420	0.72	0.0417	0.0418	0.19	0.0421	0.93
3.0	0.0356	0.0355	0.14	0.0359	0.74	0.0356	0.0356	0.11	0.0359	0.88
4.0	0.0327	0.0325	0.43	0.0337	3.12	0.0327	0.0325	0.46	0.0339	3.65
5.0	0.0311	0.0310	0.29	0.0316	1.61	0.0311	0.0311	0.29	0.0318	2.23
6.0	0.0303	0.0302	0.26	0.0315	3.91	0.0303	0.0302	0.23	0.0318	4.80
7.0	0.0299	0.0298	0.37	0.0302	1.10	0.0299	0.0298	0.37	0.0305	2.01
8.0	0.0297	0.0296	0.30	0.0299	0.70	0.0297	0.0296	0.34	0.0300	0.96
9.0	0.0297	0.0296	0.24	0.0300	0.84	0.0297	0.0296	0.27	0.0300	0.88
10.0	0.0298	0.0298	0.13	0.0299	0.25	0.0298	0.0298	0.17	0.0299	0.24

E (MeV)	VTTi5					VTAg1				
0.1	0.7986	0.8492	6.14	0.8535	6.64	0.8818	0.9373	6.10	0.9382	6.20
0.2	0.1991	0.2146	7.49	0.2164	8.34	0.2097	0.2267	7.79	0.2263	7.61
0.3	0.1237	0.1306	5.43	0.1320	6.49	0.1265	0.1342	5.91	0.1342	5.88
0.4	0.0985	0.1021	3.63	0.1042	5.62	0.0995	0.1035	3.98	0.1041	4.59
0.5	0.0854	0.0877	2.67	0.0882	3.23	0.0858	0.0883	2.93	0.0885	3.17
0.6	0.0770	0.0785	1.95	0.0791	2.64	0.0770	0.0787	2.17	0.0790	2.49
0.8	0.0660	0.0669	1.26	0.0679	2.87	0.0658	0.0668	1.40	0.0671	1.83
1.0	0.0587	0.0592	0.88	0.0613	4.37	0.0585	0.0591	1.00	0.0594	1.57
2.0	0.0417	0.0418	0.22	0.0424	1.58	0.0416	0.0417	0.24	0.0421	1.22
3.0	0.0356	0.0356	0.11	0.0368	3.43	0.0357	0.0356	0.11	0.0359	0.73
4.0	0.0327	0.0325	0.43	0.0340	3.92	0.0329	0.0328	0.43	0.0331	0.51
5.0	0.0311	0.0311	0.29	0.0319	2.45	0.0315	0.0314	0.29	0.0321	1.75
6.0	0.0303	0.0302	0.26	0.0331	8.81	0.0308	0.0307	0.26	0.0313	1.70
7.0	0.0299	0.0298	0.37	0.0311	4.11	0.0305	0.0304	0.33	0.0310	1.69
8.0	0.0297	0.0296	0.30	0.0302	1.55	0.0304	0.0303	0.30	0.0308	1.41
9.0	0.0297	0.0296	0.24	0.0301	1.28	0.0305	0.0304	0.23	0.0307	0.83
10.0	0.0298	0.0298	0.13	0.0299	0.36	0.0306	0.0306	0.13	0.0305	0.33

Table 2. (Continued.)

E (MeV)	VTTi1					VTTi2				
	XCOM	XMuDat	Δa	MCNPX	Δb	XCOM	XMuDat	Δa	MCNPX	Δb
E (MeV)	VTAg2					VTAg3				
0.1	0.9288	0.9874	6.12	0.9870	6.07	0.9781	1.0400	6.13	1.0439	6.50
0.2	0.2157	0.2336	7.97	0.2354	8.73	0.2220	0.2408	8.12	0.2397	7.66
0.3	0.1282	0.1363	6.12	0.1378	7.23	0.1300	0.1385	6.33	0.1383	6.16
0.4	0.1001	0.1044	4.21	0.1043	4.13	0.1007	0.1052	4.37	0.1056	4.74
0.5	0.0860	0.0887	3.08	0.0886	3.01	0.0863	0.0891	3.24	0.0894	3.55
0.6	0.0771	0.0789	2.29	0.0793	2.75	0.0772	0.0791	2.43	0.0794	2.74
0.8	0.0658	0.0668	1.49	0.0673	2.27	0.0658	0.0668	1.57	0.0675	2.69
1.0	0.0584	0.0590	1.06	0.0596	2.04	0.0583	0.0590	1.13	0.0597	2.37
2.0	0.0415	0.0417	0.26	0.0422	1.68	0.0415	0.0416	0.29	0.0425	2.30
3.0	0.0358	0.0357	0.08	0.0360	0.73	0.0358	0.0358	0.08	0.0361	0.83
4.0	0.0331	0.0330	0.42	0.0334	0.82	0.0333	0.0332	0.39	0.0335	0.59
5.0	0.0318	0.0317	0.25	0.0322	1.18	0.0321	0.0320	0.25	0.0322	0.57
6.0	0.0311	0.0311	0.23	0.0315	1.14	0.0315	0.0314	0.22	0.0316	0.34
7.0	0.0309	0.0308	0.32	0.0312	1.03	0.0313	0.0312	0.35	0.0313	0.06
8.0	0.0309	0.0308	0.32	0.0311	0.83	0.0313	0.0312	0.32	0.0312	0.37
9.0	0.0310	0.0309	0.23	0.0309	0.27	0.0315	0.0314	0.22	0.0310	1.61
10.0	0.0312	0.0312	0.13	0.0308	1.14	0.0318	0.0317	0.13	0.0309	2.81
E (MeV)	VTAg4					VTAg5				
0.1	1.0270	1.0930	6.23	1.0939	6.30	1.079	1.147	6.11	1.149	6.28
0.2	0.2283	0.2480	8.27	0.2468	7.78	0.2348	0.2555	8.44	0.2545	8.04
0.3	0.1317	0.1406	6.54	0.1405	6.44	0.1336	0.1429	6.73	0.1434	7.07
0.4	0.1014	0.1061	4.53	0.1065	4.89	0.1021	0.1071	4.78	0.1080	5.62
0.5	0.0865	0.0895	3.40	0.0900	3.92	0.0868	0.0899	3.55	0.0911	4.83
0.6	0.0773	0.0793	2.55	0.0798	3.23	0.0774	0.0795	2.69	0.0800	3.28
0.8	0.0657	0.0668	1.66	0.0677	3.03	0.0657	0.0668	1.75	0.0679	3.44
1.0	0.0582	0.0589	1.20	0.0597	2.59	0.0581	0.0588	1.25	0.0599	3.01
2.0	0.0415	0.0416	0.31	0.0426	2.62	0.0414	0.0416	0.31	0.0430	3.63
3.0	0.0359	0.0359	0.06	0.0362	0.80	0.0360	0.0360	0.06	0.0374	3.77
4.0	0.0335	0.0334	0.39	0.0335	0.16	0.0337	0.0336	0.39	0.0343	1.78
5.0	0.0323	0.0323	0.28	0.0324	0.08	0.0326	0.0326	0.25	0.0336	2.81
6.0	0.0318	0.0318	0.22	0.0317	0.48	0.0322	0.0321	0.22	0.0319	0.95
7.0	0.0317	0.0316	0.32	0.0313	1.15	0.0321	0.0320	0.34	0.0316	1.75
8.0	0.0318	0.0317	0.28	0.0313	1.54	0.0323	0.0322	0.28	0.0315	2.54
9.0	0.0320	0.0320	0.22	0.0310	3.16	0.0326	0.0325	0.22	0.0314	3.68
10.0	0.0323	0.0323	0.12	0.0310	4.24	0.0329	0.0329	0.12	0.0313	5.21
E (MeV)	VTPb1					VTPb2				
0.1	0.8346	0.8870	6.09	0.8893	6.34	1.037	1.096	5.53	1.099	5.76
0.2	0.2037	0.2198	7.60	0.2196	7.53	0.2354	0.2540	7.60	0.2563	8.51
0.3	0.1249	0.1321	5.60	0.1322	5.64	0.1354	0.1438	6.02	0.1439	6.06
0.4	0.0988	0.1027	3.83	0.1032	4.27	0.1036	0.1081	4.25	0.1086	4.71
0.5	0.0855	0.0879	2.78	0.0900	5.07	0.0881	0.0909	3.15	0.0914	3.68
0.6	0.0770	0.0786	2.04	0.0790	2.56	0.0785	0.0804	2.42	0.0809	3.09
0.8	0.0659	0.0668	1.33	0.0674	2.33	0.0665	0.0675	1.55	0.0678	1.87
1.0	0.0586	0.0591	0.93	0.0599	2.19	0.0588	0.0595	1.12	0.0599	1.74
2.0	0.0416	0.0417	0.22	0.0417	0.18	0.0417	0.0418	0.29	0.0417	0.03
3.0	0.0356	0.0356	0.11	0.0415	15.27	0.0359	0.0358	0.08	0.0416	14.79
4.0	0.0327	0.0326	0.43	0.0361	9.72	0.0332	0.0330	0.42	0.0362	8.64
5.0	0.0313	0.0312	0.29	0.0329	5.21	0.0318	0.0317	0.25	0.0331	4.11
6.0	0.0305	0.0304	0.23	0.0317	4.13	0.0311	0.0311	0.23	0.0318	2.28
7.0	0.0301	0.0300	0.37	0.0309	2.54	0.0309	0.0308	0.32	0.0310	0.47
8.0	0.0299	0.0299	0.30	0.0308	2.69	0.0308	0.0307	0.29	0.0308	0.12
9.0	0.0300	0.0299	0.23	0.0304	1.53	0.0309	0.0309	0.23	0.0307	0.61

Table 2. (Continued.)

E (MeV)	VTTi1					VTTi2				
	XCOM	XMuDat	Δa	MCNPX	Δb	XCOM	XMuDat	Δa	MCNPX	Δb
10.0	0.0301	0.0301	0.13	0.0303	0.80	0.0311	0.0311	0.13	0.0305	2.19

E (MeV)	VTPb3					VTPb4				
0.1	1.227	1.293	5.24	1.295	5.42	1.417	1.490	5.02	1.493	5.25
0.2	0.2656	0.2865	7.57	0.2880	8.09	0.2958	0.3190	7.55	0.3181	7.27
0.3	0.1454	0.1550	6.39	0.1549	6.30	0.1555	0.1662	6.65	0.1667	6.94
0.4	0.1082	0.1133	4.60	0.1147	5.87	0.1128	0.1186	5.01	0.1193	5.62
0.5	0.0906	0.0938	3.46	0.0942	3.87	0.0931	0.0966	3.74	0.0969	4.05
0.6	0.0800	0.0822	2.74	0.0826	3.19	0.0815	0.0840	3.05	0.0843	3.44
0.8	0.0671	0.0683	1.74	0.0690	2.72	0.0678	0.0691	1.93	0.0694	2.39
1.0	0.0591	0.0599	1.24	0.0603	1.96	0.0594	0.0603	1.39	0.0605	1.88
2.0	0.0418	0.0420	0.36	0.0420	0.58	0.0419	0.0421	0.40	0.0423	1.03
3.0	0.0361	0.0361	0.03	0.0419	14.76	0.0364	0.0364	0.03	0.0419	14.19
4.0	0.0336	0.0334	0.39	0.0364	8.24	0.0339	0.0338	0.35	0.0367	7.73
5.0	0.0323	0.0322	0.25	0.0333	2.92	0.0328	0.0328	0.24	0.0334	1.58
6.0	0.0318	0.0317	0.22	0.0320	0.67	0.0324	0.0323	0.22	0.0322	0.60
7.0	0.0316	0.0315	0.32	0.0310	1.65	0.0323	0.0322	0.31	0.0311	3.56
8.0	0.0316	0.0315	0.29	0.0310	1.90	0.0324	0.0323	0.28	0.0310	4.30
9.0	0.0318	0.0317	0.22	0.0309	2.73	0.0326	0.0326	0.21	0.0310	5.13
10.0	0.0321	0.0320	0.12	0.0306	4.70	0.0330	0.0329	0.09	0.0307	7.22

E (MeV)	VTPb5					VTPb6				
0.1	1.619	1.700	4.88	1.569	3.12	1.8210	1.9090	4.72	1.9143	5.00
0.2	0.3275	0.3532	7.55	0.3333	1.75	0.3592	0.3874	7.55	0.3868	7.40
0.3	0.1660	0.1780	6.98	0.1734	4.37	0.1765	0.1897	7.21	0.1890	6.83
0.4	0.1176	0.1240	5.30	0.1244	5.60	0.1224	0.1295	5.64	0.1299	5.92
0.5	0.0957	0.0996	4.06	0.0988	3.22	0.0982	0.1026	4.38	0.1031	4.89
0.6	0.0830	0.0859	3.38	0.0867	4.36	0.0845	0.0877	3.68	0.0878	3.81
0.8	0.0684	0.0699	2.14	0.0700	2.36	0.0690	0.0707	2.33	0.0712	3.16
1.0	0.0597	0.0606	1.55	0.0608	1.91	0.0600	0.0610	1.70	0.0613	2.30
2.0	0.0420	0.0422	0.45	0.0427	1.65	0.0421	0.0423	0.52	0.0430	2.13
3.0	0.0366	0.0366	0.00	0.0420	13.68	0.0369	0.0369	0.05	0.0375	1.54
4.0	0.0344	0.0343	0.32	0.0368	6.89	0.0348	0.0347	0.32	0.0350	0.73
5.0	0.0334	0.0333	0.24	0.0335	0.20	0.0339	0.0339	0.21	0.0340	0.31
6.0	0.0330	0.0330	0.18	0.0323	2.11	0.0337	0.0336	0.18	0.0330	2.17
7.0	0.0330	0.0329	0.27	0.0312	5.55	0.0338	0.0337	0.27	0.0320	5.52
8.0	0.0332	0.0332	0.24	0.0312	6.47	0.0341	0.0340	0.23	0.0315	8.04
9.0	0.0336	0.0335	0.21	0.0311	7.85	0.0345	0.0345	0.20	0.0313	9.69
10.0	0.0340	0.0340	0.09	0.0308	9.92	0.0350	0.0350	0.09	0.0310	12.10

E (MeV)	VTBi1					VTBi2				
0.1	0.8346	0.8870	6.09	0.8898	6.41	0.9533	1.0100	5.78	1.0146	6.23
0.2	0.2037	0.2198	7.60	0.2193	7.39	0.2219	0.2396	7.67	0.2398	7.74
0.3	0.1249	0.1321	5.60	0.1319	5.48	0.1308	0.1388	5.93	0.1391	6.17
0.4	0.0988	0.1027	3.83	0.1031	4.22	0.1015	0.1057	4.05	0.1062	4.56
0.5	0.0855	0.0879	2.78	0.0890	4.04	0.0869	0.0896	3.01	0.0901	3.56
0.6	0.0770	0.0786	2.04	0.0789	2.50	0.0778	0.0795	2.25	0.0801	3.01
0.8	0.0659	0.0668	1.33	0.0678	2.89	0.0662	0.0672	1.47	0.0687	3.69
1.0	0.0586	0.0591	0.93	0.0592	1.13	0.0587	0.0593	1.03	0.0600	2.32
2.0	0.0416	0.0417	0.22	0.0418	0.56	0.0416	0.0417	0.26	0.0430	3.15
3.0	0.0356	0.0356	0.11	0.0414	15.18	0.0357	0.0357	0.08	0.0421	16.29
4.0	0.0327	0.0326	0.43	0.0358	8.88	0.0330	0.0329	0.39	0.0359	8.38
5.0	0.0313	0.0312	0.29	0.0328	4.93	0.0316	0.0315	0.29	0.0329	4.07
6.0	0.0305	0.0304	0.23	0.0314	2.90	0.0309	0.0308	0.23	0.0328	5.99
7.0	0.0301	0.0300	0.37	0.0307	2.03	0.0306	0.0305	0.33	0.0319	4.16
8.0	0.0299	0.0299	0.30	0.0310	3.62	0.0305	0.0304	0.33	0.0322	5.47

Table 2. (Continued.)

E (MeV)	VTTi1					VTTi2				
	XCOM	XMuDat	Δa	MCNPX	Δb	XCOM	XMuDat	Δa	MCNPX	Δb
9.0	0.0300	0.0299	0.23	0.0300	0.25	0.0306	0.0305	0.23	0.0311	1.68
10.0	0.0301	0.0301	0.13	0.0297	1.43	0.0308	0.0307	0.13	0.0309	0.38

E (MeV)	VTBi3					VTBi4				
0.1	1.0600	1.1210	5.59	1.0216	3.69	1.1790	1.2440	5.37	1.2469	5.60
0.2	0.2386	0.2576	7.66	0.2597	8.48	0.2569	0.2774	7.67	0.2787	8.16
0.3	0.1363	0.1450	6.19	0.1470	7.52	0.1422	0.1516	6.40	0.1537	7.76
0.4	0.1040	0.1086	4.33	0.1107	6.28	0.1066	0.1116	4.58	0.1113	4.29
0.5	0.0882	0.0911	3.21	0.0916	3.77	0.0896	0.0928	3.42	0.0933	3.99
0.6	0.0786	0.0805	2.43	0.0808	2.80	0.0794	0.0815	2.62	0.0818	3.09
0.8	0.0665	0.0676	1.58	0.0688	−3.38	0.0668	0.0680	1.72	0.0689	3.07
1.0	0.0588	0.0595	1.13	0.0601	2.28	0.0589	0.0596	1.23	0.0602	2.15
2.0	0.0417	0.0418	0.29	0.0438	5.06	0.0417	0.0418	0.34	0.0439	5.14
3.0	0.0359	0.0359	0.06	0.0422	16.20	0.0360	0.0360	0.06	0.0423	15.93
4.0	0.0332	0.0331	0.39	0.0368	10.32	0.0335	0.0333	0.39	0.0369	9.82
5.0	0.0319	0.0318	0.25	0.0336	5.29	0.0323	0.0322	0.25	0.0339	4.86
6.0	0.0313	0.0312	0.22	0.0330	5.30	0.0317	0.0316	0.22	0.0331	4.34
7.0	0.0310	0.0309	0.32	0.0326	5.03	0.0315	0.0314	0.32	0.0326	3.47
8.0	0.0310	0.0309	0.29	0.0325	4.87	0.0315	0.0314	0.32	0.0325	3.09
9.0	0.0311	0.0310	0.23	0.0321	3.03	0.0317	0.0316	0.22	0.0323	1.90
10.0	0.0313	0.0313	0.13	0.0311	0.66	0.0320	0.0319	0.13	0.0312	2.46

E (MeV)	VTBi5					VTBi6				
0.1	1.2980	1.3670	5.18	1.3705	5.44	1.4640	1.5390	5.00	1.5440	5.32
0.2	0.2751	0.2972	7.72	0.2973	7.75	0.3009	0.3251	7.73	0.3234	7.22
0.3	0.1482	0.1583	6.59	0.1578	6.29	0.1566	0.1679	6.96	0.1668	6.32
0.4	0.1093	0.1147	4.82	0.1154	5.41	0.1131	0.1191	5.17	0.1196	5.57
0.5	0.0910	0.0944	3.64	0.0949	4.15	0.0931	0.0968	3.91	0.0970	4.18
0.6	0.0802	0.0824	2.82	0.0827	3.18	0.0813	0.0839	3.07	0.0843	3.57
0.8	0.0671	0.0684	1.86	0.0693	3.22	0.0676	0.0689	2.02	0.0703	3.96
1.0	0.0590	0.0598	1.33	0.0600	1.68	0.0592	0.0601	1.46	0.0615	3.80
2.0	0.0417	0.0419	0.38	0.0440	5.30	0.0418	0.0420	0.43	0.0444	6.14
3.0	0.0362	0.0362	0.03	0.0424	15.85	0.0364	0.0364	0.00	0.0432	17.11
4.0	0.0337	0.0336	0.39	0.0370	9.32	0.0341	0.0340	0.35	0.0339	0.62
5.0	0.0326	0.0325	0.22	0.0340	4.17	0.0331	0.0330	0.24	0.0343	3.54
6.0	0.0321	0.0320	0.19	0.0333	3.62	0.0327	0.0326	0.21	0.0336	2.66
7.0	0.0320	0.0319	0.31	0.0327	2.24	0.0327	0.0326	0.31	0.0332	1.82
8.0	0.0321	0.0320	0.28	0.0326	1.61	0.0328	0.0327	0.27	0.0329	0.29
9.0	0.0323	0.0323	0.19	0.0324	0.32	0.0332	0.0331	0.21	0.0326	1.78
10.0	0.0327	0.0326	0.12	0.0314	3.75	0.0335	0.0335	0.12	0.0321	4.24

Δa = [(XCOM − XMuDat)/((XCOM + XMuDat)/2)] × 100.
Δb = [(XCOM − MCNPX)/((XCOM + MCNPX)/2)] × 100.

statement [20]:

$$\text{HVL} = \frac{\ln(2)}{\mu}. \quad (2)$$

The theoretical μ_m values were computed via XCOM program in terms of the weight fraction of the individual element (w_i) based on the following equation [21, 22]:

$$\mu_m = \sum_i w_i (\mu_m)_i. \quad (3)$$

The following equations were employed to compute the percentage difference (Δ) of the data according to XCOM,

MCNPX Monte Carlo and XMuDat models;

$$\Delta^a = \left| \left[\frac{(XCOM - XMuDat)}{\frac{(XCOM + XMuDat)}{2}} \right] \times 100 \right| \% \quad (4)$$

$$\Delta^a = \left| \left[\frac{(XCOM - MCNPX)}{\frac{(XCOM + MCNPX)}{2}} \right] \times 100 \right| \%. \quad (5)$$
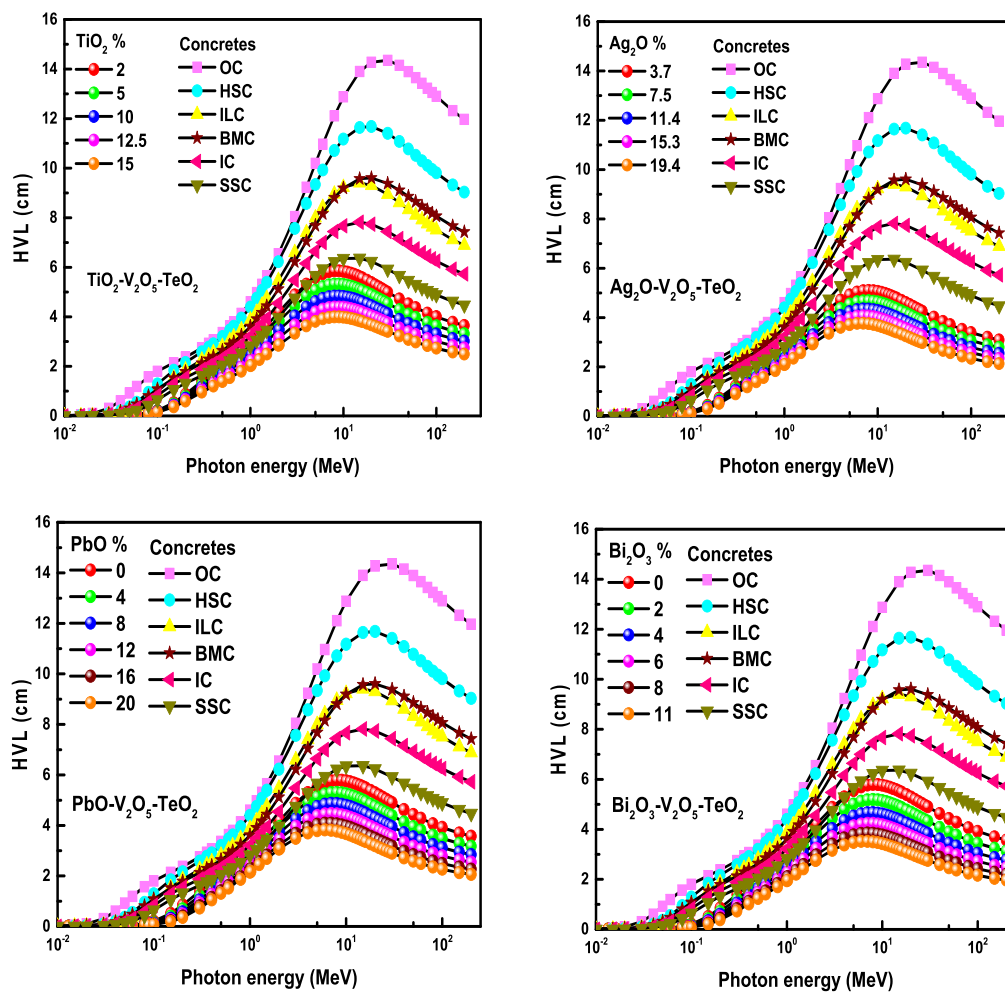
Figure 5. HVL values for VTTi, VTAg, VTPb and VTBi glass systems with various types of concrete.
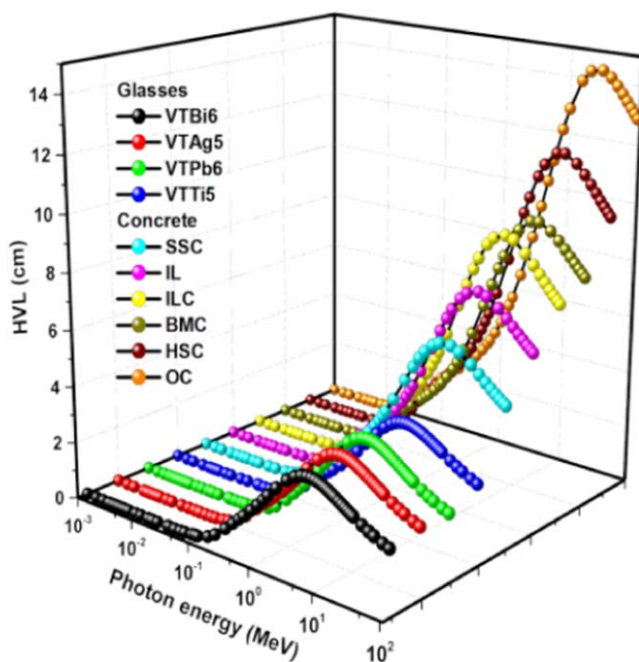

Figure 6. Half value layer for the VTTi5, VTAg5, VTPb6 and VTBi6 glass samples comparable to the HVL values of different types of concretes.
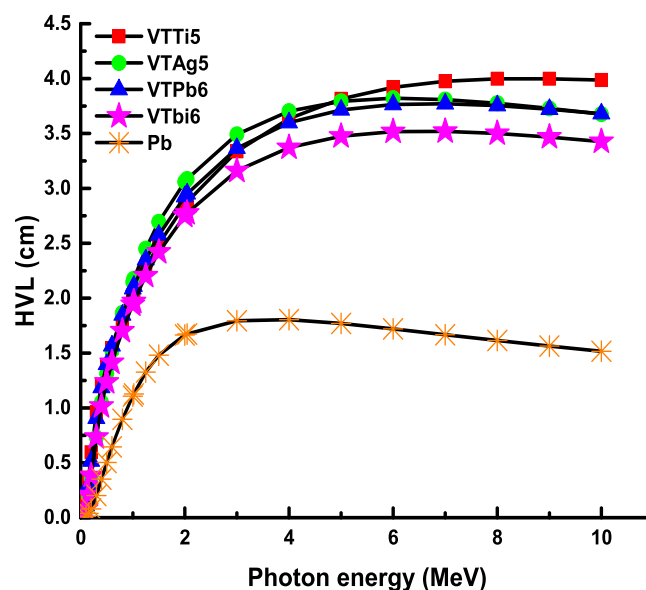

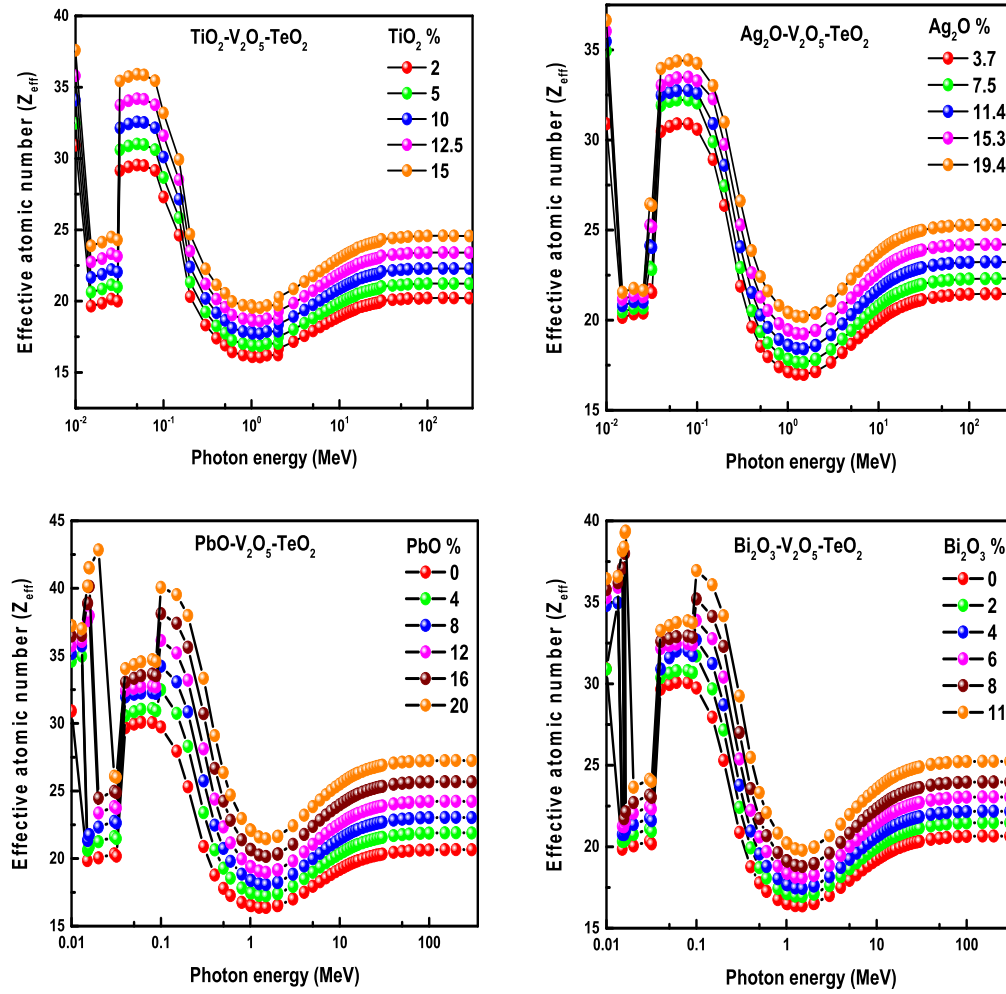**Figure 7.** Half value layer for VTTi5, VTAg5, VTPb6 and VTBi6 glass samples comparable to the HVL values of lead (Pb).

Figure 8. Variation of effective atomic number values as a function of photon energy for VTTi, VTAg, VTPb and VTBi glass samples.

The μ_m values are also used to compute the total atomic cross-section (σ_a) [23]:

$$\sigma_a = \frac{\mu_m}{N_A \sum_i^n (w_i / A_i)},$$ (6)

where N_A and A_i are Avogadro's number, and atomic weight of the individual element. In addition, the total electronic cross-section of the element (σ_e) is calculated using [23]:

$$\sigma_e = \frac{1}{N_A} \sum_i^n \frac{f_i A_i}{Z_i} (\mu_m)_i,$$ (7)

where f_i and Z_i are the number of element atoms i proportional to the total number of atoms of all elements in the glass sample. Hence, the effective atomic number (Z_{eff}) of the glass is calculated using σ_a and σ_e as follows [23]:

$$Z_{eff} = \frac{\sigma_a}{\sigma_e}.$$ (8)

Mathematically the electron density (N_{el}) (electron g^{-1}) can be calculated using μ_m and σ_e values as follows:

$$N_{el} = \frac{\mu_m}{\sigma_e}.$$ (9)

The EABF, ΣR, MCNPX code, XCOM and XMuDat program have been discussed in details in previous works [12, 24, 18, 25–28].

Results and discussions

Figures 2(A)–(D) underlines the μ_m values for photon energies of VTTi, VTAg, VTPb, and VTBi glass systems. It is clear that the value of μ_m is a maximum in the low photon energy 0.1 MeV for the whole glass series. With 0.015 MeV of an incident photon, where the predominant is the photoelectric effect (PE), the values of μ_m are ranged from 0.7986 to 0.7992 g cm^{-2} for VTTi glasses, from 0.8818 to 1.079 g cm^{-2} for VTAg glasses, from 0.8346 to 1.8210 g cm^{-2} for VTPb glasses and from 0.8346 to 1.4640 g cm^{-2} for VTBi glasses. Therefore, the μ_m values for the whole glasses decrement fast with an increment of incident photon energy. As the energy was ranged from 0.3 to 3 MeV, wherever Compton effect is the predominant process, the magnitudes of μ_m of all glass samples differ in a slight range. As the incident photon energy exceeds 3 MeV, the μ_m values for the whole explored glass samples performs similarity and can be treated as a constant,

Table 3. Effective atomic number for all glass samples.

E (MeV)	VTTi1	VTTi2	VTTi3	VTTi4	VTTi5	VTAg1	VTAg2	VTAg3	VTAg4	VTAg5
0.010	30.92	32.47	34.09	35.80	37.59	30.90	34.95	35.47	36.04	36.65
0.015	19.65	20.63	21.67	22.75	23.89	20.15	20.45	20.80	21.16	21.55
0.020	19.85	20.85	21.89	22.98	24.13	20.35	20.66	21.02	21.37	21.77
0.030	19.99	20.99	22.04	23.14	24.30	21.68	22.94	24.14	25.28	26.45
0.032	29.15	30.61	32.14	33.75	35.43	21.54	22.81	24.04	25.19	26.36
0.040	29.41	30.88	32.42	34.04	35.75	30.48	31.91	32.48	33.03	33.97
0.050	29.54	31.02	32.57	34.20	35.91	30.75	32.14	32.64	33.30	34.23
0.060	29.50	30.98	32.53	34.15	35.86	30.90	32.22	32.74	33.45	34.38
0.080	29.17	30.63	32.16	33.76	35.45	30.89	32.22	32.75	33.49	34.43
0.100	27.30	28.67	30.10	31.61	33.19	30.60	32.05	32.60	33.28	34.25
0.150	24.62	25.85	27.15	28.50	29.93	28.92	29.90	30.91	32.29	33.02
0.200	20.32	21.33	22.40	23.52	24.69	26.37	27.45	28.60	29.76	30.99
0.300	18.32	19.24	20.20	21.21	22.27	21.89	22.92	24.08	25.29	26.62
0.400	17.40	18.27	19.18	20.14	21.15	19.62	20.52	21.54	22.63	23.86
0.500	16.91	17.76	18.64	19.58	20.56	18.55	19.36	20.28	21.28	22.42
0.600	16.44	17.26	18.12	19.03	19.98	17.97	18.74	19.60	20.54	21.62
0.800	16.22	17.03	17.88	18.77	19.71	17.41	18.13	18.93	19.81	20.81
1.000	16.20	17.01	17.86	18.76	19.70	17.15	17.84	18.62	19.47	20.44
1.022	16.09	16.90	17.74	18.63	19.56	17.14	17.82	18.59	19.44	20.41
1.250	16.08	16.88	17.73	18.61	19.54	17.00	17.67	18.43	19.27	20.22
1.500	16.21	17.02	17.87	18.76	19.70	16.98	17.65	18.41	19.23	20.19
2.000	16.22	17.03	17.89	18.78	19.72	17.14	17.81	18.58	19.42	20.38
2.044	16.68	17.51	18.39	19.31	20.27	17.15	17.83	18.60	19.44	20.40
3.000	17.16	18.02	18.92	19.86	20.86	17.66	18.37	19.18	20.07	21.07
4.000	17.57	18.45	19.38	20.34	21.36	18.20	18.94	19.79	20.69	21.73
5.000	17.91	18.80	19.74	20.73	21.76	18.66	19.43	20.30	21.23	22.28
6.000	18.19	19.10	20.05	21.06	22.11	19.03	19.81	20.69	21.64	22.71
7.000	18.42	19.34	20.31	21.33	22.39	19.33	20.13	21.02	21.98	23.05
8.000	18.62	19.55	20.53	21.55	22.63	19.58	20.39	21.30	22.26	23.33
9.000	18.79	19.73	20.72	21.75	22.84	19.79	20.61	21.51	22.47	23.56
10.000	18.93	19.88	20.87	21.92	23.01	19.97	20.79	21.71	22.67	23.75
11.000	19.06	20.01	21.02	22.07	23.17	20.12	20.95	21.87	22.84	23.93
12.000	19.17	20.13	21.14	22.19	23.30	20.26	21.09	22.02	22.99	24.07
13.000	19.26	20.23	21.24	22.30	23.42	20.38	21.21	22.13	23.11	24.20
14.000	19.34	20.31	21.33	22.39	23.51	20.48	21.31	22.24	23.21	24.30
15.000	19.41	20.39	21.40	22.47	23.60	20.56	21.40	22.32	23.30	24.40
16.000	19.53	20.50	21.53	22.60	23.73	20.63	21.47	22.40	23.38	24.47
18.000	19.62	20.60	21.63	22.71	23.85	20.75	21.60	22.52	23.50	24.59
20.000	19.70	20.69	21.72	22.81	23.95	20.85	21.69	22.62	23.60	24.69
22.000	19.76	20.75	21.79	22.88	24.02	20.93	21.78	22.70	23.69	24.78
24.000	19.82	20.81	21.85	22.94	24.09	21.00	21.85	22.77	23.75	24.85
26.000	19.86	20.85	21.89	22.99	24.14	21.06	21.90	22.83	23.81	24.91
28.000	19.90	20.89	21.94	23.04	24.19	21.10	21.95	22.87	23.86	24.95
30.000	20.02	21.02	22.08	23.18	24.34	21.14	21.99	22.91	23.89	24.99
40.000	20.09	21.10	22.15	23.26	24.42	21.26	22.12	23.05	24.03	25.12
50.000	20.13	21.14	22.19	23.30	24.47	21.33	22.18	23.11	24.10	25.18
60.000	20.18	21.19	22.25	23.36	24.53	21.37	22.22	23.15	24.13	25.22
80.000	20.20	21.21	22.27	23.38	24.55	21.42	22.27	23.20	24.18	25.26
100.00	20.22	21.23	22.29	23.41	24.58	21.44	22.29	23.22	24.19	25.28

Energy (MeV)	VTPb1	VTPb2	VTPb3	VTPb4	VTPb5	VTPb6	VTBi1	VTBi2	VTBi3	VTBi4	VTBi5	VTBi6
0.010	30.92	34.60	35.17	35.74	36.47	37.24	30.92	30.90	34.80	35.28	35.78	36.45
0.015	19.85	34.98	35.74	36.06	36.51	37.01	19.85	34.98	34.97	35.92	36.20	36.59
0.020	20.05	20.63	21.35	37.60	38.87	40.16	20.05	20.33	20.76	21.25	37.09	38.17
0.030	20.35	20.63	21.34	37.67	38.90	40.15	20.35	20.33	20.75	21.23	21.72	38.39
0.032	20.18	20.86	21.77	37.98	40.11	41.54	20.18	20.45	20.98	21.55	38.00	39.28
0.040	29.68	20.86	21.76	37.98	40.14	41.50	29.68	20.45	20.98	21.55	22.14	39.37
0.050	29.95	21.25	22.33	23.37	24.47	42.84	29.95	20.75	21.37	22.06	22.72	23.65

Table 3. (Continued.)

E (MeV)	VTTi1	VTTi2	VTTi3	VTTi4	VTTi5	VTAg1	VTAg2	VTAg3	VTAg4	VTAg5		
0.060	30.09	21.62	22.76	23.84	24.98	26.10	30.09	21.11	21.76	22.46	23.17	24.14
0.080	30.07	21.48	22.63	23.73	24.87	26.01	30.07	20.94	21.60	22.32	23.03	24.01
0.100	29.74	30.57	31.96	32.43	33.04	34.06	29.74	30.38	30.91	32.17	32.60	33.27
0.150	27.95	30.85	32.16	32.61	33.34	34.36	27.95	30.65	31.60	32.34	32.78	33.57
0.200	25.30	31.05	32.25	32.72	33.53	34.56	25.30	30.81	32.01	32.44	32.89	33.76
0.300	20.89	31.10	32.28	32.77	33.66	34.72	20.89	30.81	32.02	32.46	32.93	33.87
0.400	18.77	30.94	32.21	32.70	33.53	34.58	18.77	30.69	31.73	32.39	32.86	33.74
0.500	17.79	32.49	34.23	36.14	38.13	40.07	17.79	31.71	32.69	33.89	35.20	36.95
0.600	17.27	30.75	33.07	35.21	37.41	39.54	17.27	29.69	31.24	32.77	34.13	36.08
0.800	16.76	28.31	30.85	33.20	35.63	37.99	16.76	27.16	28.71	30.41	32.30	34.18
1.000	16.52	23.39	25.75	28.11	30.72	33.34	16.52	22.42	23.78	25.39	27.01	29.25
1.022	16.51	20.64	22.47	24.40	26.67	29.10	16.51	19.93	20.96	22.23	23.57	25.48
1.250	16.39	19.28	20.75	22.33	24.25	26.36	16.39	18.72	19.56	20.60	21.72	23.33
1.500	16.37	18.54	19.80	21.16	22.84	24.70	16.37	18.07	18.79	19.70	20.68	22.10
2.000	16.51	17.82	18.85	19.97	21.38	22.96	16.51	17.44	18.04	18.81	19.64	20.83
2.044	16.52	17.48	18.40	19.42	20.69	22.13	16.52	17.14	17.68	18.39	19.15	20.24
3.000	17.00	17.45	18.37	19.37	20.64	22.07	17.00	17.12	17.66	18.36	19.11	20.19
4.000	17.50	17.28	18.13	19.07	20.26	21.61	17.50	16.97	17.48	18.14	18.86	19.88

Energy (MeV)	VTPb1	VTPb2	VTPb3	VTPb4	VTPb5	VTPb6	VTBi1	VTBi2	VTBi3	VTBi4	VTBi5	VTBi6
5.000	17.94	17.24	18.07	18.98	20.15	21.46	17.94	16.94	17.44	18.09	18.78	19.79
6.000	18.28	17.39	18.23	19.15	20.32	21.63	18.28	17.09	17.59	18.25	18.96	19.97
7.000	18.58	17.41	18.25	19.17	20.34	21.66	18.58	17.11	17.61	18.27	18.97	19.99
8.000	18.82	17.94	18.84	19.82	21.05	22.43	18.82	17.62	18.15	18.86	19.61	20.68
9.000	19.03	18.50	19.45	20.48	21.78	23.21	19.03	18.17	18.73	19.47	20.27	21.38
10.000	19.20	18.99	19.98	21.05	22.38	23.85	19.20	18.64	19.23	20.01	20.82	21.98
11.000	19.34	19.37	20.39	21.48	22.84	24.33	19.34	19.01	19.61	20.41	21.25	22.43
12.000	19.47	19.69	20.73	21.84	23.22	24.72	19.47	19.31	19.94	20.75	21.61	22.80
13.000	19.59	19.96	21.01	22.14	23.52	25.04	19.59	19.57	20.21	21.03	21.90	23.10
14.000	19.69	20.17	21.23	22.37	23.77	25.29	19.69	19.78	20.43	21.26	22.13	23.34
15.000	19.77	20.35	21.43	22.57	23.99	25.51	19.77	19.97	20.61	21.46	22.34	23.55
16.000	19.84	20.51	21.60	22.75	24.17	25.70	19.84	20.12	20.78	21.62	22.51	23.74
18.000	19.96	20.65	21.75	22.91	24.32	25.87	19.96	20.26	20.92	21.77	22.66	23.90
20.000	20.05	20.78	21.87	23.04	24.46	26.02	20.05	20.38	21.04	21.90	22.79	24.04
22.000	20.14	20.88	21.99	23.15	24.58	26.14	20.14	20.48	21.15	22.01	22.91	24.15
24.000	20.20	20.97	22.08	23.25	24.69	26.24	20.20	20.56	21.24	22.10	23.00	24.25
26.000	20.25	21.05	22.16	23.34	24.78	26.33	20.25	20.64	21.32	22.18	23.09	24.34
28.000	20.29	21.17	22.29	23.47	24.91	26.46	20.29	20.76	21.44	22.31	23.22	24.47
30.000	20.33	21.27	22.39	23.58	25.02	26.58	20.33	20.86	21.54	22.41	23.33	24.58
40.000	20.46	21.35	22.48	23.67	25.12	26.67	20.46	20.95	21.63	22.50	23.41	24.68
50.000	20.53	21.42	22.55	23.74	25.19	26.74	20.53	21.01	21.70	22.57	23.48	24.75
60.000	20.57	21.48	22.61	23.80	25.25	26.81	20.57	21.07	21.76	22.63	23.55	24.81
80.000	20.62	21.53	22.66	23.85	25.30	26.86	20.62	21.12	21.80	22.68	23.59	24.86
100.000	20.64	21.57	22.70	23.89	25.34	26.91	20.64	21.15	21.84	22.72	23.63	24.90

that may stem from the process of pair production (PP) is the dominance [13]. Based on figures 2(A)–(D); the μ_m values increase as the contents of TiO_2 changes from 2 to 15 mol% in VTTi glass system, Ag_2O changes from 3.7 to 19.4 mol% in VTAg, PbO changes from 0 to 20 mol% in VTPb glass system and Bi_2O_3 changes from 0 to 11 mol% in VTBi glasses. Moreover, the presented curves in figures 2(A)–(D) displayed peaks at 4.95, 5.46, 31.81, 88 and 90.53 keV for the k-absorption edge of Ti, Ag, Te, Pb, and Bi, respectively. The collected μ_m values according to XCOM data are compared

with the gathered data from MCNPX code (version 2.4.0) and XMuDat software as shown in figures 2(A)–(D). The calculated values of μ_m according XCOM data, MCNPX code (version 2.4.0), XMuDat and their percentage difference are listed in table 2 and as shown in figure 3.

The analysis of the whole glass systems revealed specific glasses had the highest values of μ_m according to figure 3. These glasses are VTTi5, VTAg5, VTPb6 and VTBi6, respectively. The values maximum of μ_m these glasses are compared to the values of μ_m for OC, hematite-serpentine
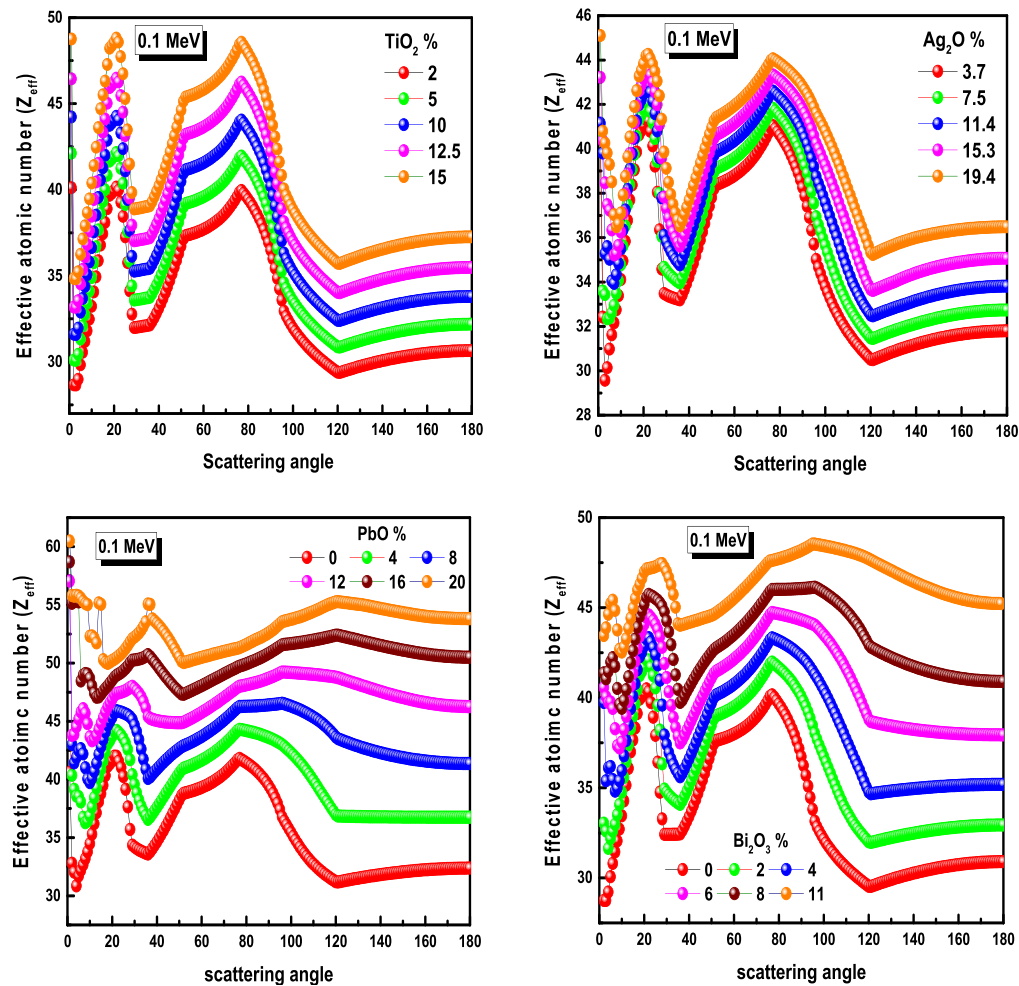
Figure 9. The variation in effective atomic numbers with scattering angles at 0.1.

(HSC), ilmenite-limonite (ILC), basalt-magnetite (BMC), ilmenite (IC), and steel-scrap (SSC) [19]. As shown in figure 4, the lowest μ_m values are recorded for OC while the highest values are recorded for the VTBi6 glass sample. That underlines the outperforming radiation shielding effectiveness of VTBi6 glass samples compared to the other investigated mentioned materials.

As shown in figure 5, the HVL results of the studied glass systems increase up to its maximum around (9 MeV) and then decrease as the photon energy increases. The HVL values of all glass samples are lower than for OC, HSC, ILC, BMC, IC, and SSC concretes. Figure 6 displays the HVL values for the highest amount of TiO$_2$, Ag$_2$O, PbO and Bi$_2$O$_3$ in the studied glass systems. The glass samples that had optimum HVL are 15TiO$_2$–35V$_2$O$_5$–50TeO$_2$, 19.4Ag$_2$O–24.7V$_2$O$_5$–55.9TeO$_2$, 20PbO–24V$_2$O$_5$–56TeO$_2$ and 11Bi$_2$O$_3$–27V$_2$O$_5$–62TeO$_2$, respectively in order to compare. As depicted in figure 6, when comparing the HVL values of the explored glasses with that of other materials, the lowest HVL values are recorded for 11Bi$_2$O$_3$–27V$_2$O$_5$–62TeO$_2$ glass sample while the highest values are recorded for OC. It means that the 11Bi$_2$O$_3$–27V$_2$O$_5$–62TeO$_2$ glass sample shows better radiation shielding capability compared to further explored glasses and materials. Figure 7 shows

the half value layer of our glass samples (VTTi, VTAg, VTPb, and VTBi) relative HVL of lead (Pb).

The considered Z_{eff} values for various photon energy levels of the whole glass systems VTTi, VTAg, VTPb, and VTBi are given in figure 8. The figure implies that all, the whole explored glasses had a high value of Z_{eff} at lowest energy level 0.01 MeV. For the VTTi glass system, the magnitudes of Z_{eff} vary from 20.21–30.92, 21.22–32.47, 22.28–34.09, 23.39–35.79 and 24.56–37.58 for VTTi1, VTTi2, VTTi3, VTTi4, and VTTi5 glass samples, respectively. For the VTAg glass system, the Z_{eff} values had ranged from 21.45–30.89, 22.29–34.94, 23.22–35.47, 24.19–36.06 and 25.28–36.64 for VTAg1, VTAg2, VTAg3, VTAg4, and VTAg5 glass samples, respectively. For the VTPb glass system, the magnitudes of Z_{eff} are varying from 20.65–30.91, 21.89–34.60, 23.03–35.16, 24.22–35.74, 25.68–36.45 and 27.24–37.24 for VTPb1, VTPb2, VTPb3, VTPb4, VTPb5 and VTPb6 glass samples, respectively. For the VTBi glass system, the magnitudes of Z_{eff} are varying from 20.65–30.91, 21.47–30.89, 22.16–34.79, 23.05–35.28, 23.96–35.78 and 25.23–36.44 for VTBi1, VTBi2, VTBi3, VTBi4, VTBi5 and VTBi6 glass samples respectively. According to the preceding data, it is revealed that the magnitudes of Z_{eff} are

Table 4. Equivalent atomic number (Z_{eq}) for investigated glass samples.

Energy (MeV)	VTTi1	VTTi2	VTTi3	VTTi4	VTTi5	VTAg1	VTAg2	VTAg3	VTAg4	VTAg5
0.015	21.31	21.30	21.29	21.29	21.28	21.74	21.98	22.24	22.50	22.77
0.020	21.51	21.50	21.49	21.48	21.48	21.92	22.15	22.39	22.64	22.90
0.030	21.81	21.81	21.79	21.79	21.78	23.71	25.25	26.71	28.06	29.37
0.040	35.65	35.64	35.64	35.64	35.63	37.25	38.16	39.10	39.99	40.94
0.050	36.24	36.24	36.24	36.22	36.22	37.83	38.71	39.63	40.52	41.43
0.060	36.67	36.67	36.67	36.66	36.65	38.25	39.13	40.01	40.88	41.78
0.080	37.23	37.22	37.22	37.22	37.21	38.79	39.64	40.50	41.34	42.21
0.100	37.62	37.61	37.60	37.60	37.60	39.15	39.99	40.84	41.66	42.51
0.150	38.21	38.21	38.21	38.21	38.19	39.70	40.50	41.32	42.12	42.93
0.200	38.54	38.54	38.54	38.54	38.52	40.01	40.80	41.62	42.39	43.16
0.300	38.97	38.96	38.94	38.98	38.97	40.40	41.18	41.96	42.68	43.46
0.400	39.19	39.19	39.18	39.18	39.17	40.61	41.38	42.10	42.85	43.60
0.500	39.32	39.32	39.31	39.29	39.31	40.74	41.49	42.24	42.97	43.70
0.600	39.40	39.42	39.39	39.39	39.39	40.83	41.57	42.31	43.04	43.76
0.800	39.48	39.52	39.52	39.52	39.51	40.92	41.63	42.40	43.12	43.81
1.000	39.50	39.50	39.50	39.49	39.56	40.92	41.70	42.42	43.08	43.85
1.500	37.54	37.68	37.67	37.53	37.67	39.21	40.11	41.02	41.85	42.67
2.000	33.51	33.61	33.50	33.60	33.50	35.71	36.76	37.87	38.91	40.08
3.000	30.11	30.17	30.16	30.10	30.15	32.18	33.37	34.64	35.89	37.16
4.000	29.05	29.00	28.99	29.03	29.03	31.08	32.24	33.52	34.88	36.22
5.000	28.50	28.50	28.48	28.52	28.52	30.50	31.72	32.96	34.29	35.63
6.000	28.17	28.15	28.18	28.14	28.17	30.15	31.35	32.65	33.96	35.28
8.000	27.76	27.76	27.74	27.76	27.76	29.72	30.92	32.22	33.54	34.84
10.000	27.57	27.59	27.57	27.58	27.58	29.51	30.75	32.05	33.30	34.65
15.000	27.51	27.51	27.52	27.49	27.51	29.45	30.67	31.94	33.20	34.59

Energy (MeV)	VTPb1	VTPb2	VTPb3	VTPb4	VTPb5	VTPb6	VTBi1	VTBi2	VTBi3	VTBi4	VTBi5	VTBi6
0.015	21.50	22.40	23.20	23.96	24.82	25.67	21.50	22.04	22.51	23.04	23.55	24.25
0.020	21.69	23.16	24.46	25.69	26.92	28.11	21.69	22.53	23.27	24.02	24.79	25.83
0.030	21.99	23.55	24.92	26.19	27.46	28.65	21.99	22.88	23.67	24.47	25.24	26.32
0.040	36.33	37.33	38.09	38.89	39.86	40.85	36.33	37.16	37.76	38.58	39.39	40.38
0.050	36.93	37.90	38.66	39.40	40.36	41.32	36.93	37.74	38.33	39.14	39.93	40.89
0.060	37.35	38.32	39.07	39.81	40.75	41.68	37.35	38.16	38.76	39.56	40.33	41.28
0.080	37.91	38.87	39.61	40.34	41.26	42.18	37.91	38.72	39.31	40.08	40.85	41.80
0.100	38.29	41.61	44.34	46.84	49.31	51.66	38.29	40.31	41.97	43.73	45.38	47.54
0.150	38.87	42.42	45.31	47.92	50.46	52.80	38.87	41.01	42.78	44.59	46.30	48.51
0.200	39.21	42.89	45.89	48.54	51.10	53.45	39.21	41.43	43.25	45.12	46.85	49.09
0.300	39.63	43.50	46.57	49.32	51.90	54.28	39.63	41.95	43.85	45.73	47.54	49.81
0.400	39.83	43.80	46.97	49.77	52.38	54.76	39.83	42.24	44.18	46.10	47.96	50.26
0.500	39.98	44.05	47.27	50.08	52.70	55.08	39.98	42.41	44.42	46.37	48.20	50.53
0.600	40.07	44.19	47.46	50.28	52.92	55.29	40.07	42.55	44.57	46.56	48.38	50.70
0.800	40.13	44.35	47.65	50.50	53.16	55.53	40.13	42.68	44.74	46.75	48.56	50.93
1.000	40.15	44.38	47.74	50.57	53.25	55.64	40.15	42.75	44.78	46.84	48.62	51.00
1.500	38.35	42.61	46.05	49.17	51.94	54.47	38.35	41.05	43.01	45.27	47.16	49.72
2.000	34.33	38.57	42.02	45.13	48.27	51.02	34.33	36.92	38.99	41.23	43.22	46.05
3.000	30.97	34.12	36.93	39.72	42.70	45.59	30.97	32.90	34.61	36.54	38.45	40.97
4.000	29.84	32.60	35.12	37.65	40.38	43.14	29.84	31.58	33.07	34.89	36.69	38.99
5.000	29.29	31.86	34.23	36.60	39.26	41.95	29.29	30.94	32.35	34.04	35.70	38.04
6.000	28.92	31.39	33.74	35.95	38.60	41.22	28.92	30.54	31.89	33.59	35.18	37.42
8.000	28.54	30.87	33.05	35.28	37.76	40.37	28.54	30.08	31.35	32.96	34.53	36.77
10.000	28.34	30.69	32.76	34.91	37.41	39.95	28.34	29.82	31.13	32.68	34.25	36.40
15.000	28.25	30.55	32.59	34.71	37.13	39.59	28.25	29.71	31.04	32.53	34.07	36.18

Table 5. G-P energy absorption buildup factor coefficients (EABF).

Energy (MeV)	VTTi5					VTAg5				
	b	*c*	*a*	Xk	*d*	*b*	*c*	*a*	Xk	*d*
0.015	1.006	0.816	−0.105	8.743	0.168	1.006	1.067	−0.256	7.686	0.230
0.020	1.015	0.340	0.267	13.153	−0.209	1.013	0.312	0.284	14.846	−0.238
0.030	1.047	0.348	0.242	14.772	−0.161	1.034	0.395	0.242	11.833	−0.175
0.040	1.289	0.352	0.147	24.210	−0.153	1.458	0.325	0.113	23.373	−0.062
0.050	1.258	0.172	0.005	10.134	0.017	1.371	0.063	−0.139	8.470	0.112
0.060	1.251	0.140	0.597	14.770	−0.176	1.324	0.028	0.791	14.904	−0.190
0.080	1.282	0.184	0.457	14.154	−0.194	1.303	0.080	0.578	14.046	−0.228
0.100	1.250	0.338	0.270	15.473	−0.144	1.204	0.240	0.351	13.764	−0.182
0.150	1.620	0.360	0.267	13.949	−0.154	1.446	0.303	0.305	14.070	−0.169
0.200	2.355	0.392	0.272	13.895	−0.174	2.177	0.303	0.319	14.013	−0.197
0.300	2.495	0.632	0.135	13.805	−0.088	2.294	0.539	0.168	14.013	−0.101
0.400	2.700	0.781	0.086	13.586	−0.077	2.588	0.687	0.116	13.901	−0.091
0.500	2.681	0.889	0.051	13.481	−0.056	2.620	0.802	0.076	13.893	−0.069
0.600	2.622	0.944	0.034	13.237	−0.047	2.592	0.864	0.055	13.753	−0.057
0.800	2.465	1.006	0.015	12.858	−0.035	2.466	0.942	0.032	13.653	−0.043
1.000	2.330	1.035	0.006	12.514	−0.028	2.342	0.980	0.020	13.538	−0.035
1.500	1.944	1.109	−0.015	11.916	−0.013	1.939	1.088	−0.010	13.487	−0.016
2.000	1.841	1.088	−0.011	10.883	−0.013	1.848	1.056	−0.001	12.617	−0.022
3.000	1.678	1.032	0.004	12.369	−0.022	1.704	0.984	0.023	12.899	−0.044
4.000	1.542	1.016	0.010	14.078	−0.029	1.577	0.950	0.036	13.744	−0.056
5.000	1.455	0.989	0.020	14.148	−0.037	1.517	0.904	0.055	13.944	−0.073
6.000	1.384	0.982	0.023	14.308	−0.039	1.451	0.892	0.062	14.141	−0.078
8.000	1.293	0.959	0.035	14.030	−0.047	1.384	0.876	0.073	14.169	−0.087
10.000	1.230	0.958	0.039	14.303	−0.051	1.316	0.920	0.063	14.340	−0.077
15.000	1.145	0.949	0.052	14.723	−0.059	1.268	0.979	0.060	14.558	−0.074

| Energy (MeV)		VTPb6					VTBi6			
0.015	1.004	1.513	−0.525	5.803	0.341	1.005	1.301	−0.398	6.696	0.288
0.020	1.007	0.238	0.407	14.220	−0.448	1.010	0.261	0.317	18.046	−0.292
0.030	1.018	0.364	0.248	12.097	−0.179	1.026	0.324	0.251	18.038	−0.190
0.040	1.455	0.325	0.114	23.387	−0.063	1.441	0.328	0.117	23.458	−0.071
0.050	1.369	0.065	−0.136	8.503	0.110	1.360	0.074	−0.125	8.631	0.103
0.060	1.323	0.030	0.788	14.902	−0.190	1.317	0.038	0.773	14.892	−0.189
0.080	1.302	0.080	0.577	14.045	−0.228	1.299	0.085	0.568	14.045	−0.227
0.100	1.366	0.063	0.654	13.627	−0.311	1.296	0.122	0.563	13.520	−0.304
0.150	1.434	0.151	0.478	13.814	−0.257	1.440	0.205	0.403	13.902	−0.222
0.200	1.570	0.247	0.361	13.879	−0.209	1.693	0.286	0.325	13.932	−0.192
0.300	1.849	0.389	0.246	13.588	−0.141	1.927	0.458	0.204	13.825	−0.116
0.400	2.135	0.519	0.185	13.863	−0.125	2.253	0.586	0.154	13.870	−0.109
0.500	2.171	0.640	0.131	13.877	−0.095	2.343	0.699	0.110	13.871	−0.086
0.600	2.234	0.707	0.104	13.715	−0.081	2.373	0.766	0.085	13.728	−0.072
0.800	2.238	0.802	0.071	13.614	−0.063	2.329	0.854	0.056	13.627	−0.056
1.000	2.189	0.854	0.055	13.524	−0.055	2.246	0.903	0.041	13.505	−0.048
1.500	1.976	0.962	0.026	13.582	−0.041	1.918	1.037	0.004	13.654	−0.024
2.000	1.870	0.976	0.024	13.151	−0.043	1.849	1.019	0.011	13.096	−0.032
3.000	1.717	0.941	0.040	13.238	−0.064	1.717	0.962	0.032	13.147	−0.054
4.000	1.598	0.904	0.055	13.538	−0.077	1.588	0.928	0.045	13.632	−0.066
5.000	1.570	0.834	0.084	13.781	−0.102	1.538	0.876	0.067	13.879	−0.085
6.000	1.507	0.820	0.092	14.015	−0.109	1.473	0.865	0.073	14.094	−0.090
8.000	1.460	0.810	0.103	14.264	−0.117	1.411	0.852	0.084	14.204	−0.098
10.000	1.388	0.889	0.081	14.347	−0.095	1.341	0.909	0.069	14.342	−0.083
15.000	1.364	1.006	0.062	14.364	−0.081	1.300	0.988	0.061	14.493	−0.076
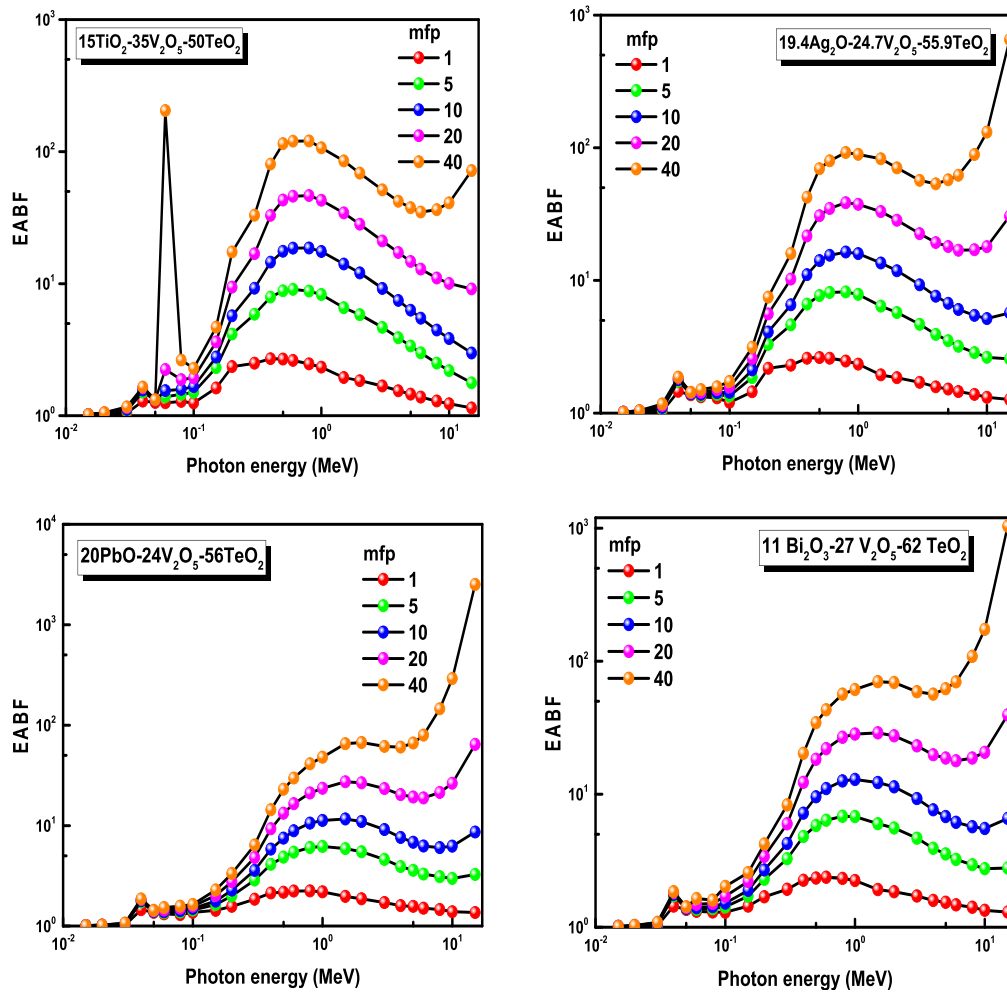
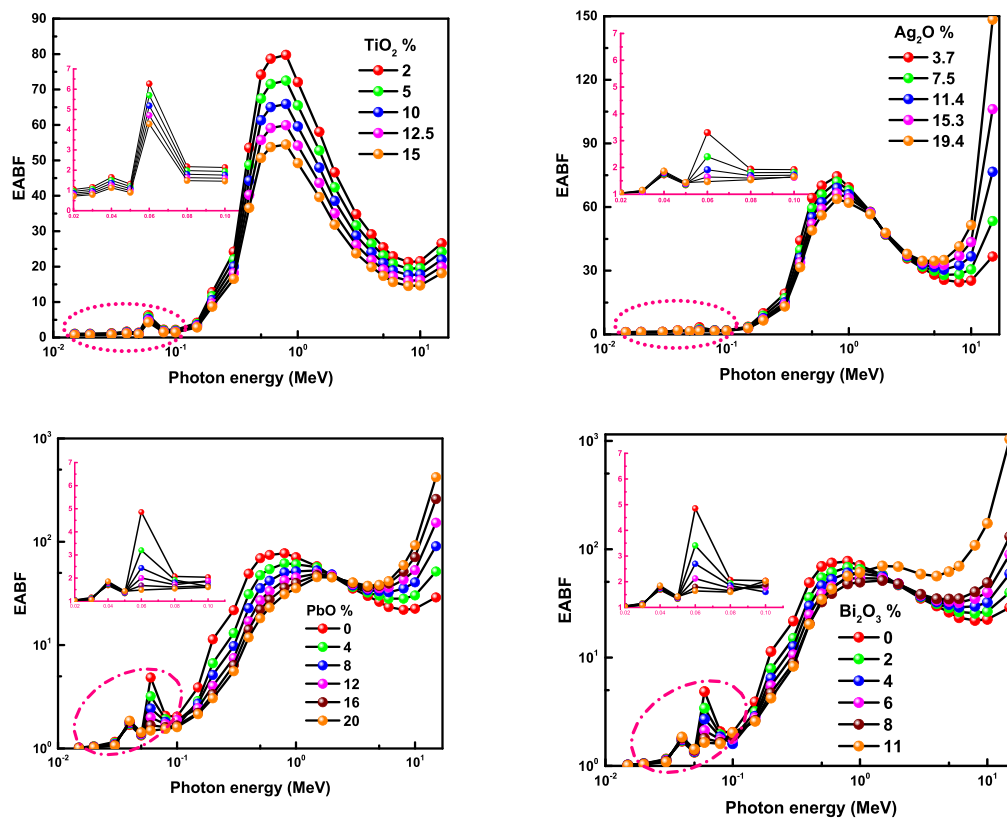**Figure 10.** Variation of energy absorption buildup factors (EABF) with photon energy for VTTi5, VTAg5, VTPb6 and VTBi6 glass samples at different penetration depths 1, 5, 10, 20 and 40 mfp.

varied as the amount of TiO$_2$ increment from 2–15 mol%, Ag$_2$O increases from 3.7 to 19.4 mol%, PbO increases from 0 to 20 mol% and the Bi$_2$O$_3$ increases from 0 to 11 mol%. Therefore, for the whole glass systems, the highest values of Z$_{eff}$ were found in the VTTi5, VTAg5, VTPb6 and VTBi6 glass samples among VTTi, VTAg, VTPb and VTBi systems, respectively. The Z$_{eff}$ values for all investigated glasses have been listed in table 3.

As the photon energy comes closer to the absorption edges of elements (Ti, V, Ag, Te, Pb, and Bi) being used in the glasses, sudden changes are observed at Z$_{eff}$ values, that stems from the remarkable changes of μ_m values at the absorption edges of each element. It was proclaimed [29] that there is a clear a satisfied photon energy- scattering angle relation that encourages researchers to calculate the values of Z$_{eff}$ theoretically. Figure 9 indicates the importance of the values of small angles upon the computation of Z$_{eff}$.

The equivalent atomic number (Z$_{eq}$) values for all glass samples are listed in table 4. While the the geometric progression (G-P) fitting parameters *a*, *b*, *c*, Xk, and *d* values for VTTi5, VTAg5, VTPb6 and VTBi6 (as examples) glass samples are listed in table 5. The G-P fitting parameters *a*, *b*, *c*, Xk, and *d* values have been computed and presented in

figure 10 for the significant explored VTTi5, VTAg5, VTPb6 and VTBi6 glass samples. The Z$_{eq'}$ values and the G-P fitting parameters had utilized to compute the EABF values for the glass samples under study. Figure 10 shows the EABF values against photon energy 0.015–15 MeV at different penetration depths for the significant explored glass samples VTTi5, VTAg5, VTPb6 and VTBi5 as an example. Due to the PE process, the EABF values of glasses are minimum in the low energy. Whereas, at intermediate energy region, the EABF values of glasses increase up to the maximum as the energy increases. This behavior may be attributed to multiple scattering by see At higher energy, there is an increment in the EABF values that is correlated to the PP process. In addition, there are sharp peaks according to the EABF-energy relation. These peaks are attributed to the edges of the K-absorption of the V, Ti, Te, Pb and Bi elements in the explored glasses. As shown in figure 10, the EABF values increase as the penetration depths increase for VTTi5, VTAg5, VTPb6 and VTBi5 glass samples. Figure 11 displays the EABF values of the studied glass samples at 30 mpf. The significant explored glass samples, VTAg5, VTPb6 and VTBi5 had the lowest EABF values in the energy range 0.015–2 MeV while the

Figure 11. Variation of energy absorption buildup factors (EABF) with photon energy for VTTi5, VTAg5, VTPb6 and VTBi6 glass samples at 30 mfp.
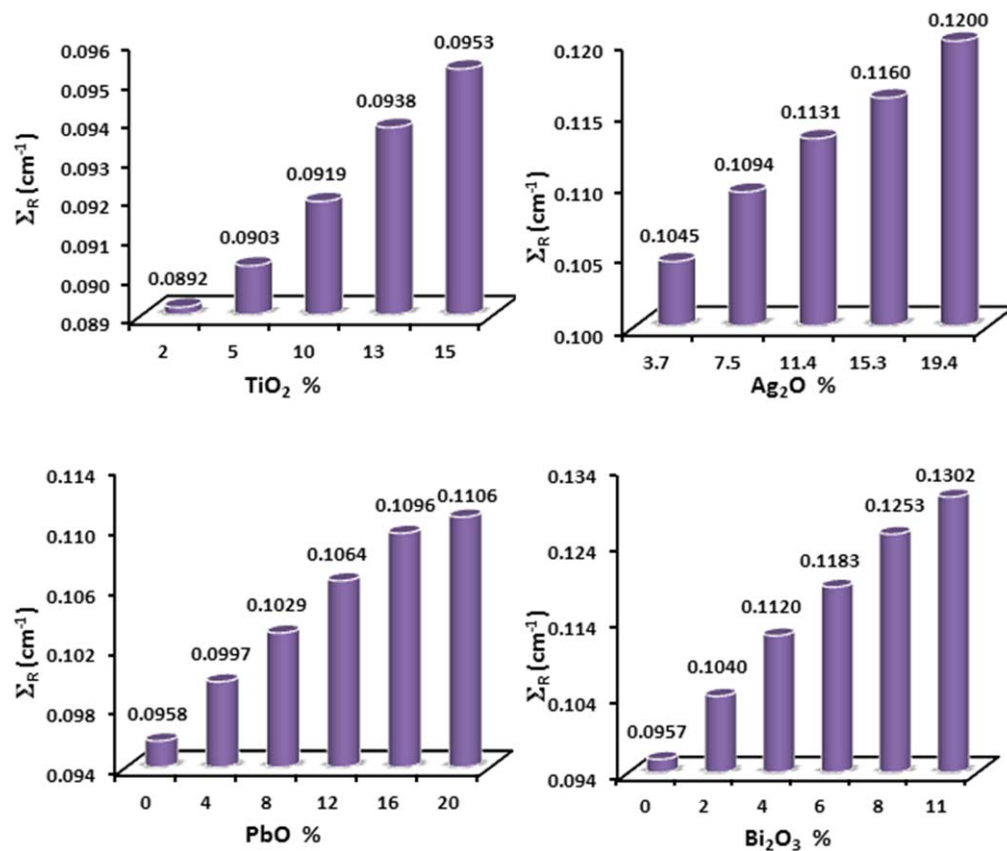

Figure 12. Fast neutron removal cross sections ΣR for the selected glass samples.
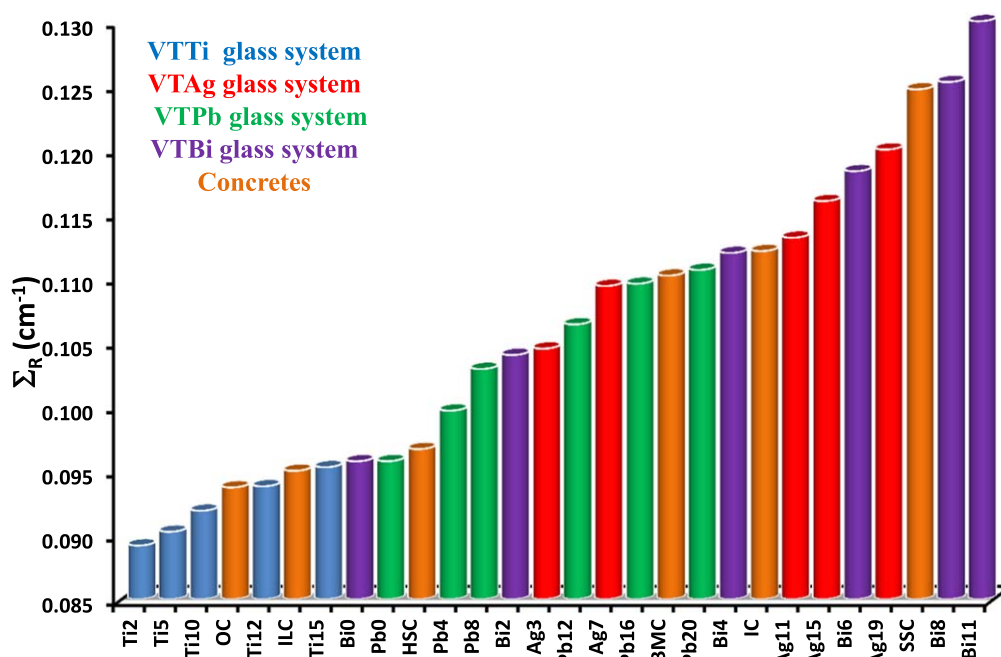
Figure 13. Fast neutron removal cross sections ΣR values for the selected glass samples compared with different concretes.
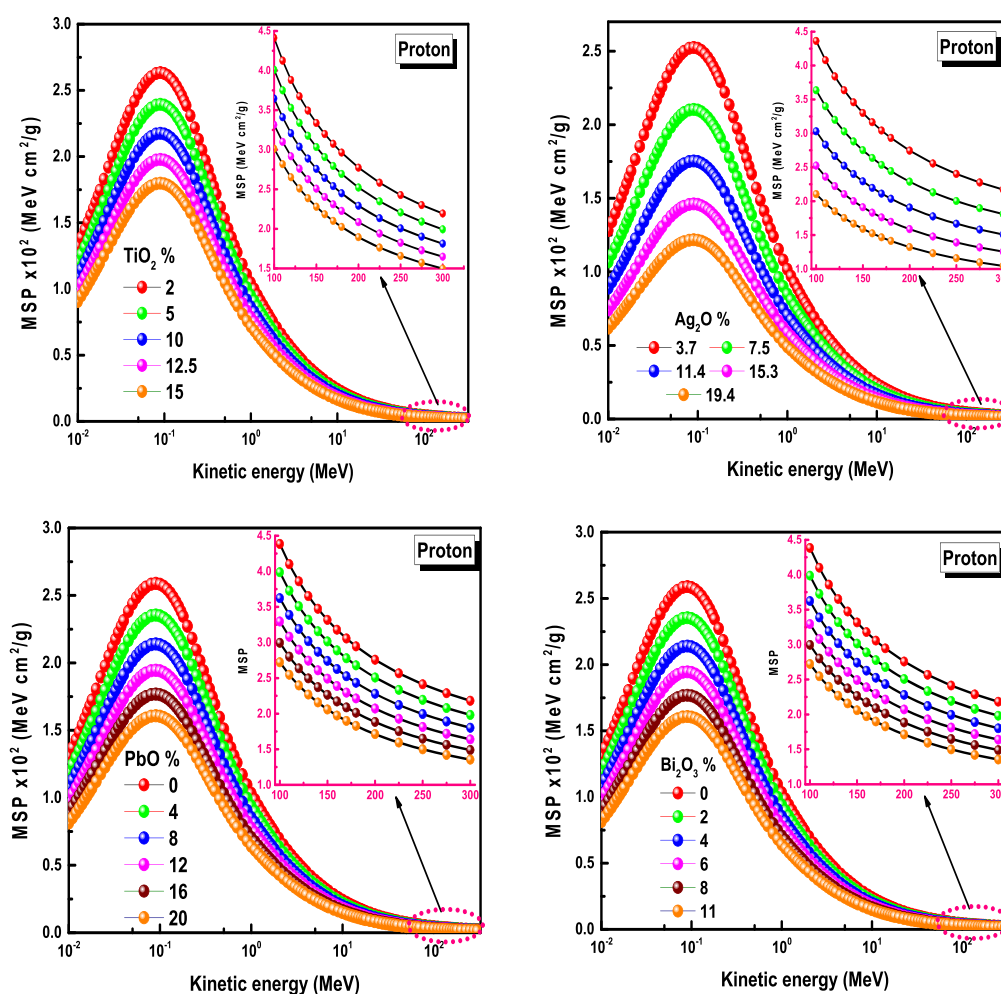

Figure 14. Variation of proton mass stopping powers as a function of kinetic energy for the selected glass samples.
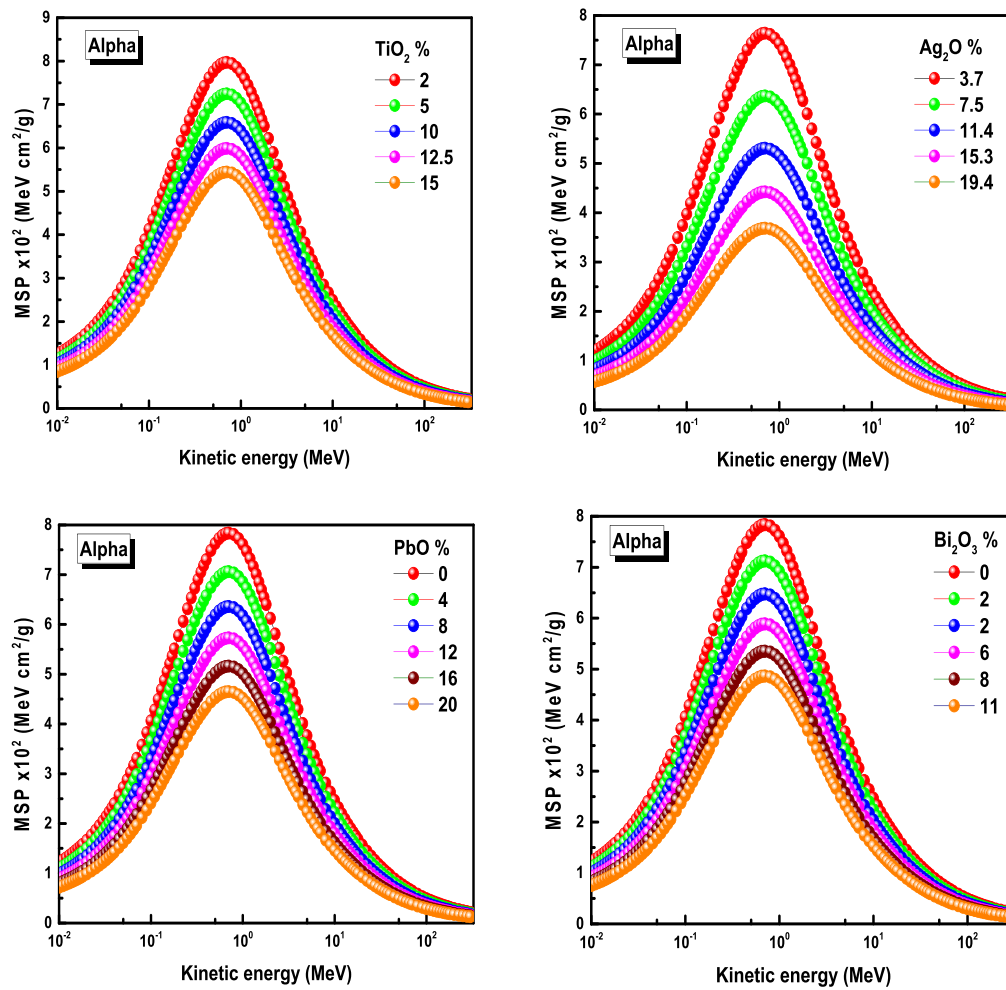
Figure 15. Variation of alpha mass stopping powers as a function of kinetic energy for the selected glass samples.

Table 6. Neutron removal cross-section $\sum R$ (cm^{-1}) for alla glass samples.

VTTi	ΣR (cm^{-1})	VTAg	ΣR (cm^{-1})	VTPb	ΣR (cm^{-1})	VTBi	ΣR (cm^{-1})
VTTi1	0.0892	VTAg1	0.1045	VTPb1	0.0958	VTBi1	0.0957
VTTi2	0.0903	VTAg2	0.1094	VTPb2	0.0997	VTBi2	0.1040
VTTi3	0.0919	VTAg3	0.1131	VTPb3	0.1029	VTBi3	0.1120
VTTi4	0.0938	VTAg4	0.1160	VTPb4	0.1064	VTBi4	0.1183
VTTi5	0.0953	VTAg5	0.1200	VTPb5	0.1096	VTBi5	0.1253
				VTPb6	0.1106	VTBi6	0.1302

glass sample VTTi5 had the lowest EABF values in the energy range 0.015–15 MeV.

Figure 12 shows that the neutron removal cross-section (ΣR) values ranged 0.0892 to 0.0953, 0.1045 to 0.1200, 0.0958 to 0.1106 and 0.0957 to 0.1302 cm^{-1} as the amount of TiO$_2$, Ag$_2$O, PbO and Bi$_2$O$_3$ increase 2–15, 3.7–19.4, 0–20 and 0–11 mol% in the VTTi, VTAg, VTPb and VTBi glass systems, respectively (see table 6). Figure 13 shows the ΣR values compared to that for various concretes. As shown in the figure, the ΣR values for the whole glass samples are higher than that of OC, except VTTi1 and VTTi2 glass samples. The ΣR values for VTTi1, VTTi2, VTTi3, VTTi4,

VTTi5, VTAg1, VTAg2, VTAg3, VTAg4, VTAg5, VTPb1, VTPb2, VTPb3, VTPb4, VTPb5, VTPb6, VTBi, VTB2, VTB3, VTB4, VTBi5 and VTBi6 glass samples are higher than that of OC, HSC, ILC concretes. Finally, the ΣR value of the VTBi6 glass sample is the highest one compared to the ΣR values of the rest of the whole investigated glass samples, OC, HSC, ILC, BMC, IC, and SSC concretes. This process implies that the VTBi6 glass sample shows the better neutron shielding effectiveness overall the rest of the investigated materials.

In the space where human beings could be exposed to protons and alpha particles, the most appropriate shielding
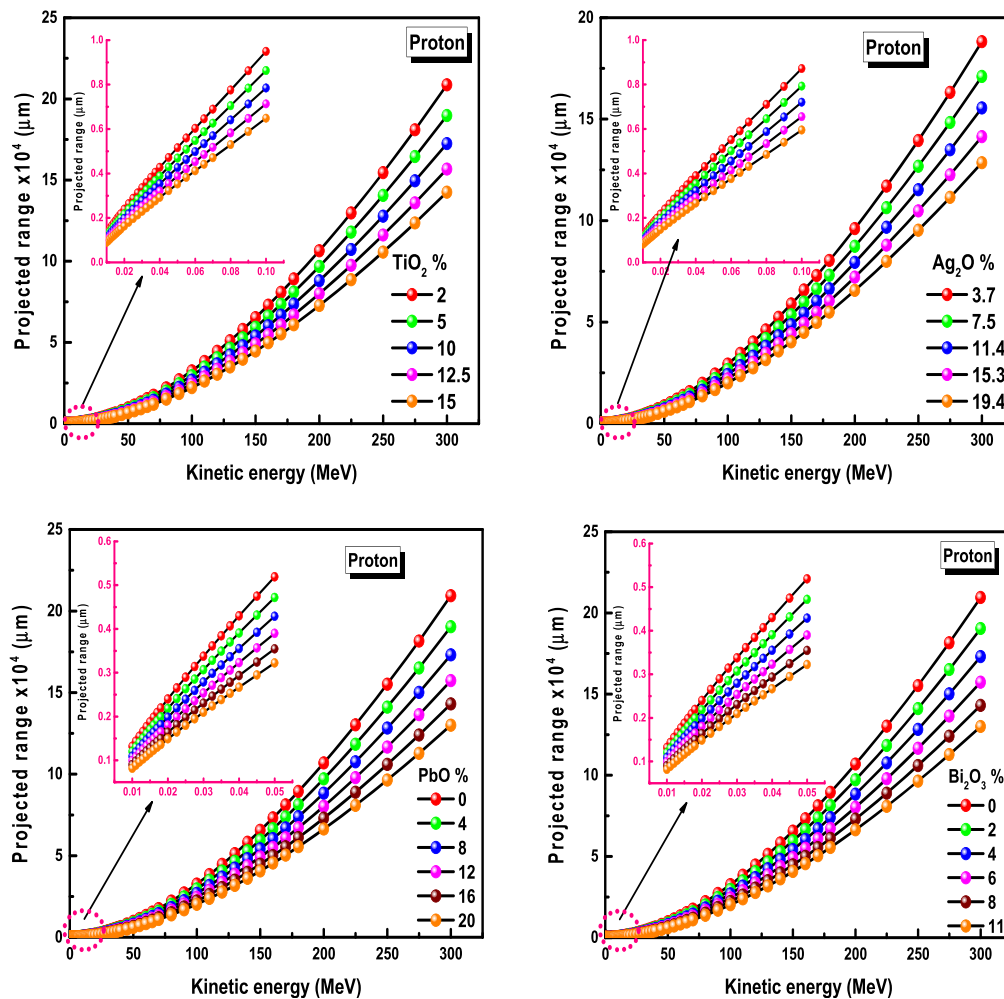
Figure 16. Variation of proton projected range as a function of kinetic energy for the selected glass samples.

materials are necessary. On the other hand, proton and alpha were used in a wide range in Hadron beam therapy. Projected range is a proper feature that can be used to investigate the nuclear radiation shielding and the interactions with various targets at various kinetic energies of protons and alpha particles. The projected range explains the mean value of the depth to which the protons and alpha particles will break through to slowing down to rest [30]. The SRIM code was used in order to calculate the proton and alpha MSP and projected range values for glass samples [31]. Figures 14, 15 show the variations of protons and alpha MSP values for different kinetic energy levels of the investigated glass samples. As seen in figures 14, 15, both the values of proton and alpha MSP increase with increasing the kinetic energy up to maximum and then decrease. Also, we can see that the lowest MPS values corresponding to the high amounts of TiO$_2$, Ag$_2$O, PbO, and Bi$_2$O$_3$ in the VTTi, VTAg, VTPb, and VTBi glass systems, respectively. As shown in figures 16, 17, the values of the proton and alpha projected range increase as a function of the kinetic energy for the whole investigated glass samples and decrease as the amount of TiO$_2$, Ag$_2$O, PbO, and Bi$_2$O$_3$ increases from 2 to 10 mol%, from 3.7 to 19.4 mol%,

from 0 to 20 mol% and from 0 to 11 mol% in the VTTi, VTAg, VTPb, and VTBi glass systems, respectively.

Conclusions

The purpose of this paper is to study different tellurovanadate based glass series in terms of their μ_m, HVL, Z_{eff}, EABF, ΣR, proton and alpha particle MSP and proton and alpha particles projected range parameters. The XCOM, MCNPX code and XMuDat program were used to calculate the μ_m. The results observed that XCOM values are mostly overlaps with both MCNPX code and XMuDat for all glass samples. At the low photon energy level, for all glass samples, both the effective atomic number and μ_m have the maximum values. The values of μ_m, HVL, and ΣR were compared to the values of OC, HSC, ILC, BMC, IC, and SSC concretes. The results underlined that 11Bi$_2$O$_3$–27V$_2$O$_5$–62TeO$_2$ glass sample has the highest values of both μ_m, and ΣR while it has the lowest values of half-value layer. The glass systems that have the highest amount of TiO$_2$, Ag$_2$O, PbO, and Bi$_2$O$_3$ recorded maximum values of Z_{eff} and minimum values of EABF, proton and alpha particle MSP as well as proton and alpha
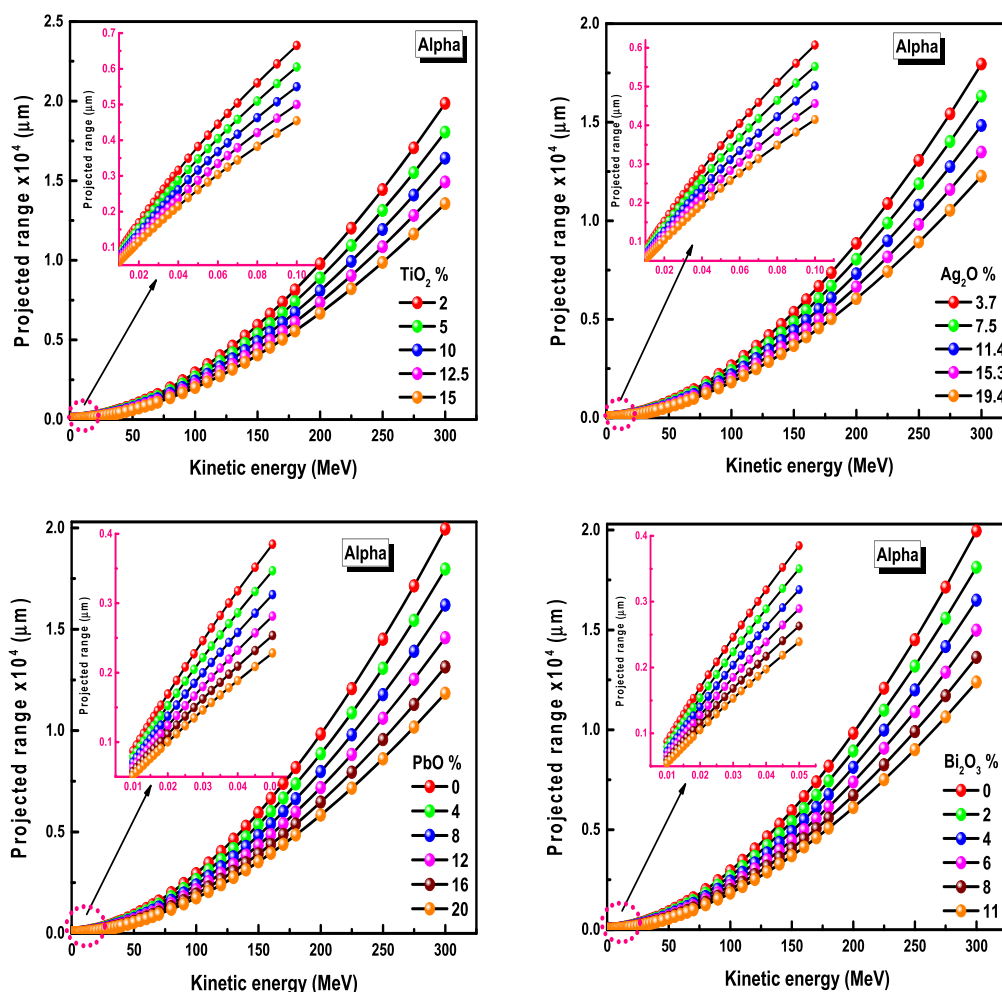
Figure 17. Variation of proton projected range as a function of kinetic energy for the selected glass samples.

particles projected range. This research paper is a valuable and promising with its unique outcomes and contributes to the following research studies focusing on shielding materials.

ORCID iDs

Yasser B Saddeek ⓘ https://orcid.org/0000-0003-3737-1035
K Aly ⓘ https://orcid.org/0000-0002-0673-6217

References

[1] Mahmoud I S, Issa S A M, Saddeek Y B, Tekin H O, Kilicoglu O, Alharbi T, Sayyed M I, Erguzel T T and Elsaman R 2019 Gamma, neutron shielding and mechanical parameters for lead vanadate glasses *Ceram. Int.* **45** 14058–72

[2] Kavaz E 2019 An experimental study on gamma ray shielding features of lithium borate glasses doped with dolomite, hematite and goethite minerals *Radiat. Phys. Chem.* **160** 112–23

[3] Tekin H O, Sayyed M I and Issa S A M 2018 Gamma radiation shielding properties of the hematite-serpentine concrete blended with WO_3 and Bi_2O_3 micro and nano particles using MCNPX code *Radiat. Phys. Chem.* **150** 95–100

[4] Kaur P, Singh K J, Thakur S, Singh P and Bajwa B S 2019 Investigation of bismuth borate glass system modified with barium for structural and gamma-ray shielding properties *Spectrochim. Acta* A **206** 367–77

[5] Waly E-S A, Al-Qous G S and Bourham M A 2018 Shielding properties of glasses with different heavy elements additives for radiation shielding in the energy range 15–300 keV *Radiat. Phys. Chem.* **150** 120–4

[6] Kurudirek M, Chutithanapanon N, Laopaiboon R, Yenchai C and Bootjomchai C 2018 Effect of Bi_2O_3 on gamma ray shielding and structural properties of borosilicate glasses recycled from high pressure sodium lamp glass *J. Alloys Compd.* **745** 355–64

[7] Issa S A M, Tekin H O, Elsaman R, Kilicoglu O, Saddeek Y B and Sayyed M I 2019 Radiation shielding and mechanical properties of Al_2O_3–Na_2O–B_2O_3–Bi_2O_3 glasses using MCNPX Monte Carlo code *Mater. Chem. Phys.* **223** 209–19

[8] Ersundu A E, Büyükyıldız M, Çelikbilek Ersundu M, Şakar E and Kurudirek M 2018 The heavy metal oxide glasses within the WO_3–MoO_3–TeO_2 system to investigate

the shielding properties of radiation applications *Prog. Nucl. Energy* **104** 280–7

[9] Yasmin S, Barua B S, Khandaker M U, Chowdhury F-U-Z, Rashid M A, Bradley D A, Olatunji M A and Kamal M 2018 Studies of ionizing radiation shielding effectiveness of silica-based commercial glasses used in Bangladeshi dwellings *Results Phys.* **9** 541–9

[10] Darwish A A A, Issa S A M and El-Nahass M M 2016 Effect of gamma irradiation on structural, electrical and optical properties of nanostructure thin films of nickel phthalocyanine *Synth. Met.* **215** 200–6

[11] Yusub S, Narendrudu T, Suresh S and Krishna Rao D 2014 Structural investigation of vanadium ions doped $Li_2OPbOB_2O_3P_2O_5$ glasses by means of spectroscopic and dielectric studies *J. Mol. Struct.* **1076** 136–46

[12] Ozan Tekin H, Sayyed M I, Manici T and Altunsoy E E 2018 Photon shielding characterizations of bismuth modified borate-silicate-tellurite glasses using MCNPX Monte Carlo code *Mater. Chem. Phys.* **211** 9–16

[13] Chanthima N, Kaewkhao J and Limsuwan P 2012 Study of photon interactions and shielding properties of silicate glasses containing Bi_2O_3, BaO and PbO in the energy region of 1 keV to 100 GeV *Ann. Nucl. Energy* **41** 119–24

[14] Souri D 2018 Optothermal properties of vanadate-tellurite oxide glasses and some suggested applications *Tellurite Glas. Smart Mater.* (Cham: Springer International Publishing) pp 67–104

[15] Singh K J, Kaur S and Kaundal R S 2014 Comparative study of gamma ray shielding and some properties of $PbO-SiO_2-Al_2O_3$ and $Bi_2O_3-SiO_2-Al_2O_3$ glass systems *Radiat. Phys. Chem.* **96** 153–7

[16] El-Mallawany R and Sayyed M I 2018 Comparative shielding properties of some tellurite glasses: I *Physica* B **539** 133–40

[17] Tijani S A, Kamal S M, Al-Hadeethi Y, Arib M, Hussein M A, Wageh S and Dim L A 2018 Radiation shielding properties of transparent erbium zinc tellurite glass system determined at medical diagnostic energies *J. Alloys Compd.* **741** 293–9

[18] Gaikwad D K, Sayyed M I, Obaid S S, Issa S A M and Pawar P P 2018 Gamma ray shielding properties of $TeO_2-ZnF_2-As_2O_3-Sm_2O_3$ glasses *J. Alloys Compd.* **765** 451–8

[19] Bashter I I 1997 Calculation of radiation attenuation coefficients for shielding concretes *Ann. Nucl. Energy* **24** 1389–401

[20] Issa S A M, Hamdalla T A and Darwish A A A 2017 Effect of $ErCl_3$ in gamma and neutron parameters for different concentration of $ErCl_3$-SiO_2 (EDFA) for the signal protection from nuclear radiation *J. Alloys Compd.* **698** 234–40

[21] Singh G, Gupta M K, Dhaliwal A S and Kahlon K S 2015 Measurement of attenuation coefficient, effective atomic number and electron density of oxides of lanthanides by using simplified ATM-method *J. Alloys Compd.* **619** 356–60

[22] Issa S, Sayyed M and Kurudirek M 2016 Investigation of gamma radiation shielding properties of some zinc tellurite glasses *J. Phys. Sci.* **27** 97–119

[23] Limkitjaroenporn P, Kaewkhao J, Limsuwan P and Chewpraditkul W 2011 Physical, optical, structural and gamma-ray shielding properties of lead sodium borate glasses *J. Phys. Chem. Solids* **72** 245–51

[24] Issa S A M, Darwish A A A and El-Nahass M M 2017 The evolution of gamma-rays sensing properties of pure and doped phthalocyanine *Prog. Nucl. Energy* **100** 276–82

[25] Sayyed M I, Issa S A M, Büyükyıldız M and Dong M 2018 Determination of nuclear radiation shielding properties of some tellurite glasses using MCNP5 code *Radiat. Phys. Chem.* **150** 1–8

[26] Kaplan M F 1989 *Concrete Radiation Shielding* (New York: Wiley)

[27] Chilton A B, Shultis J K and Faw R E 1984 *Principles of Radiation Shielding* (Englewood Cliffs, NJ: Prentice Hall)

[28] Issa S A M, Mostafa A M A and Auda S H 2018 Progress in nuclear energy radio-protective properties of some sunblock agents against ionizing radiation *Prog. Nucl. Energy* **107** 184–92

[29] Yalçın Z, İçelli O, Okutan M, Boncukçuoğlu R, Artun O and Orak S 2012 A different perspective to the effective atomic number (Z_{eff}) for some boron compounds and trommel sieve waste (TSW) with a new computer program ZXCOM *Nucl. Instrum. Methods Phys. Res. Sect.* A **686** 43–7

[30] Kurudirek M 2017 Heavy metal borate glasses: potential use for radiation shielding *J. Alloys Compd.* **727** 1227–36

[31] Ziegler J F, Ziegler M D and Biersack J P 2010 SRIM—The stopping and range of ions in matter *Nucl. Instrum. Methods Phys. Res.* B **268** 1818–23